STAR-LIKE MACROMERS FROM LIGNIN

by

Willer de Oliveira

Thesis Submitted to the Faculty of the

Virginia Polytechnic Institute and State University

in partial fulfillment of the requirements for the degree of

MASTER OF SCIENCE

in

Forest Products

APPROVED:

W.G. Glasser, Chairman

J.E. McGrath

N.G. Lewis

January, 1987

Blacksburg, Virginia

STAR-LIKE MACROMERS FROM LIGNIN

by

Willer de Oliveira

Committee Chairman: Wolfgang G. Glasser
Forest Products

(ABSTRACT)

Star-like macromers were prepared from hydroxypropyl lignin by reaction with propylene oxide. The average number of arms per macromer was controlled by partial capping with diethylsulfate, and the average arm length by the degree of chain extension with propylene oxide.

Six methods of analysis were applied for characterizing of the star-like macromers: total hydroxyl (by titration), vapor pressure osmometry, hydriotic acid/gas chromatography, ultraviolet spectroscopy, proton-nuclear magnetic resonance spectroscopy and thermal analysis.

Number average molecular weights were measured by vapor pressure osmometry. Total hydroxyl content was determined after acetylation by potentiometric titration. Based on HPL molecular weight and hydroxyl content it was estimated that the average HPL molecule generates a star-like structure ("macromer") with an average of 6 arms.

Hydriodic acid/gas chromatography proved to be the most appropriate method for the quantitative determination of the degree of capping. Based on this technique it was possible to classify star-like macromers with between two and six radiating arms per average molecule. The same method could also be applied for the determination of arm length. Two

different propoxylation reaction conditions produced macromers with an average of 2.5 and 3.5 propylene oxide units per arm.

Ultraviolet spectroscopy was the simplest and most rapid method of analysis investigated. The decrease in copolymer absorptivity coefficient was found to be related to an increase in non-UV absorbing mass after capping and/or chain extension.

Results indicated that H-NMR spectroscopy is an adequate method of analysis for star-like macromers. Macromer arm length was calculated from the ratio of signals representing the methyl group of acetyl (i.e. hydroxyl) and propoxyl functionality. Two levels of propoxylation produced star-like macromers with 2.2 - 2.5 and 3.9 - 4.0 propylene oxide units per arm.

Thermal analysis by DMTA of lignin derivative-containing blends with ethylene-vinyl acetate copolymer indicated that the glass transition behavior of the star-like macromers follows the Gordon-Taylor relationship for copolymers. Although variable, the results revealed a consistent decrease in T_g as a consequence of an increase of propylene oxide chain length.

ACKNOWLEDGEMENTS

The author wishes to express his appreciation to Dr. Wolfgang G. Glasser, his major advisor, for his encouragement, direction of this research and guidance of the author's general program of graduate study. Thanks are also given to Drs. J.E. McGrath and N.G. Lewis for serving on the author's advisory committee. Appreciation is also expressed towards Mrs. Charlotte Barnett for her help with laboratory techniques.

The financial support by the CNPq [1] graduate study and Foundation for Industrial Technology (Brazil) is gratefully acknowledged.

A very special thanks is due to Dr. C.B. Coulson and Mrs. Zofia Neufeld for their encouragement, loving care, and continuous moral support.

Finally, the author would like to dedicate this dissertation to his parents and wife, whose generosity, understanding, encouragement and support made this work possible.

---

[1] CNPq is the Brazilian equivalent of the National Science Foundation of the USA.

TABLE OF CONTENTS

TABLE OF CONTENTS
(Continued)

TABLE OF CONTENTS
(Continued)

LIST OF TABLES

LIST OF TABLES
(Continued)

LIST OF FIGURES

LIST OF FIGURES
(Continued)

GLOSSARY

a_{max}	Absorptivity coefficient at maximum absorption
CEHPL	Chain extended hydroxypropyl lignin
$DESO_4$	Diethylsulfate
DMTA	Dynamic mechanical thermal analysis
DSC	Differential scanning calorimetry
EIL	Enzymatically isolated lignin
ETPVA18	Ethylene/18% vinyl acetate copolymer
HI/GC	Hydriodic acid/gas chromatography
H-NMR	Proton nuclear magnetic resonance spectroscopy
HPL	Hydroxypropyl lignin
$\overline{M}_n$	Number-average molecular weight
MWL	Milled wood lignin
PE	Polyethylene (low density)
PMMA	Polymethylmethacrylate
PO	Propylene oxide
SM	Starting model
Tan δ	Damping factor or loss tangent
T_g	Glass transition temperature
UV	Ultraviolet
λ	Wave length
λ_{max}	Wave length at maximum absorption

I. INTRODUCTION

Lignin is the second most abundant natural polymer. It is recognized as a three-dimensional, highly branched polymer that binds cellulose fibers together in wood.

Despite years of research on lignin properties and utilization, and despite significant growth of lignin markets, lignin continues to be under-utilized as a raw material for commercial products (1). Only a small fraction of the more than 50 million tons of lignin potentially available annually from wood pulping worldwide is recovered, and most of the material in the spent liquors of pulping processes is burned in furnaces to recover both chemicals and steam (2). Apart from the use for energy generation, some lignins find application in various solid*) material systems (3). Among them, the most often mentioned are the use of lignin in thermosetting resins, in polyblends and in elastomers as antioxidant and reinforcement agents. However, the main limitation for the use of lignin in polymeric products is related to its polydisperse and multifunctional characteristics that affect mechanical properties, viscosity, cure rate and other important material characteristics (4). Thus, it was recognized that the synthesis of a more uniformly functional lignin derivative is desirable for the preparation of lignin-based engineering plastics (4).

---

*) Distinct from water-soluble lignin derivatives, especially lignosulfonates, which have captured a prominent position among industrial surfactants.

II. LITERATURE REVIEW

2.1 Introduction

Chemical modifications of lignin by reaction with alkylene oxides, also termed oxyalkylation or alkoxylation, have been studied extensively in the USA (5). Oxyalkylation of lignin produces a derivatized macromolecule with improved chemical and physical properties. Oxyalkylation results in a copolymer combining covalently high modulus lignins with a lower modulus aliphatic polyether (6). The synthesis of hydroxpropyl lignin derivatives by reaction of lignin with propylene oxide has been explored extensively because copolymerization reduces the insolubility of lignin and improves the viscoelastic properties of engineering plastics made therefrom (7-12). A wide range of synthesis conditions has been explored, and the kinetics of the reaction have been evaluated using several lignin-like model compounds as well as lignins. In previous work (9) the synthesis and characteristics of several types of hydroxyalkyl lignin derivatives have been studied from milled wood, organosolv, steam-explosion, acid (H_2SO_4) hydrolysis, and Kraft lignin which had been reacted with ethylene oxide, propylene oxide, and butylene oxide. The results indicate that these lignin derivatives show promise as prepolymers for thermoset engineering plastics.

2.2 Block Copolymers

In recent years, the emphasis in research and development and in the production of synthetic macromolecules has been directed toward the

preparation of cost-effective multicomponent polymer systems (i.e., copolymers, polyblends, and composites), rather than on the preparation of new and frequently more expensive homopolymers (13).

Multiphase polymer systems have gained importance during the past 20 years due to their unique structure-property relationship. The new materials can be obtained in the form of blends, block and graft copolymers, and all of these have the common characteristic of two or more polymeric phases in the solid state (14, 16).

Although more expensive, block and graft copolymers have advantages over simple blends. The formation of uniform polymeric blends is generally prevented by the incompatibility of polymeric chains, and it is difficult to prepare composite materials exhibiting all the desirable properties present in their respective components (16). One way of overcoming the handicap of polymer incompatibility is the formation of covalent bonds between the constituents to obtain block or graft copolymers. In addition, their molecular structure can be accurately controlled thereby producing novel materials (14). These characteristics, among others, place block copolymers in a new and important area of polymer science.

Another important aspect in the field of block copolymers concerns block architecture. This can dramatically affect the elastomeric behavior, melt rheology, and toughness in rigid materials (14). The most significant types of architecture are triblock, multiblock (or segmented) and star block arrangements due to their utility in elastoplastic or thermoplastic elastomer applications.

Star-block copolymers are macromolecules having more than one branch originating from a single site. The star sequence arrangement $(AB)_x$, where A and B denote dissimilar chemical structures, represents an important area of increasing interest for the study and development for new types of polymers (17-20). Block copolymers based on A-B-A, $(A-B)_n$ and $(AB)_x$ star shapes are responsible for an entire new technology called "thermoplastic elastomers". They are characterized by the unique property of combining both thermoplasticity with rubber like behavior. Their structures are composed of a minor fraction of a hard block (T_g or T_m above room temperature) and a major fraction of a soft block (T_g below room temperature). In these systems the hard segments consist of groups that are rigid and capable of strong intermolecular interaction, e.g., aromatic rings, urea, and urethane groups. These hard blocks can associate to form small morphological domains that serve as physical crosslinking and reinforcement sites (14, 21). The soft segments generally consist of long-chain polyesters or polyethers such as poly (ethylene oxide), poly (propylene oxide) and poly (oxytetramethylene).

2.3 Star-Like Macromers from Lignin

Hsu and Glasser (22) have shown that lignin may become a versatile competitive polyol through modification with maleic anhydride and propylene oxide. The reaction of lignin with alkylene oxides produces hydroxyalkylated lignin derivatives with glass transition temperatures (T_g) in the range of 50°C to 100°C, and this is about 50-75°C lower

than the T_g of the parent lignin. The solubility of hydroxyalkyl lignin derivatives in organic solvents increases dramatically allowing the preparation of solutions of up to 20% concentration in many organic solvents, thus suggesting an absence of gel structure typical of network polymers (9). Glasser et al. (23) prepared polyol from Kraft lignin adequate for the preparation of semi-rigid polyurethane foams. Results showed that a variety of polyurethane products formulated from this type of hydroxyalkyl lignin derivative exhibited properties comparable to commercial products. The uniformity in structure, reduction in brittleness, and considerable improvement in mechanical properties indicates that lignin-based network polyurethanes can be synthesized with controllable performance characteristics. A comparison of the polyol properties from the Kraft and carboxylated Kraft lignin showed that both solubility and viscosity of the polyester type polyol were increased (24).

Although the lignin-based polyurethanes showed high modulii and strengths, they were brittle and had poor elongation properties. They were also very sensitive to composition (4, 25). One way to modify macromolecular properties of lignin-based polyurethanes is to mix a polyol component, prior to crosslinking, with a low modulus hydroxy-terminated soft segment constituent, such as polyethylene glycol (PEG) or polybutadiene glycol (PBG) (26, 27). Uniform structure and improved mechanical properties with only minor additions of these glycols demonstrated that lignin-based thermosetting polyurethanes can be synthesized with a wide range of performance characteristics.

Even though these soft segments improved the strain behavior of the polyurethanes, they were limited by either the PEG content or phase separation (PBG) (25). One way to overcome this situation was to synthesize a chain-extended hydroxypropyl lignin (CEHPL). It can be expected that the propylene oxide chains will impart a flexible character to networks formed from the hydroxypropyl lignin. Since the HPL structure is rich in hydroxyl groups, with sometimes as many as ten OH groups per macromer, the CEHPL will present a star-like polyol architecture as is shown in Figure 1.

Kelley (25) has recently synthesized a series of chain-extended hydroxypropyl lignin derivatives. The CEHPL copolymers were characterized with regard to their chemical, modular, and thermal properties. Following crosslinking with diisocyanates, these materials were brittle glasses or soft rubbers. Kelley also observed that the length of the hydroxypropyl chains in the CEHPL's could be varied, and that affected copolymer properties. As the chain length increased from 1 to 7 propylene oxide units, the glass transition temperature decreased from +63 to -65^{o}C, and the modulus of elasticity (MOE) of crosslinked polyurethanes dropped from 1400 to 10 MPa.

The present work is to study the synthesis of a series of star-like macromers from lignin, and to develop a quantitative method of analysis with regard to number and length of arms.

The number of arms of the star-like macromers will be controlled by partial capping of HPL hydroxyl groups through reaction with some mono-functional substituent, such as diethylsulfate, as shown

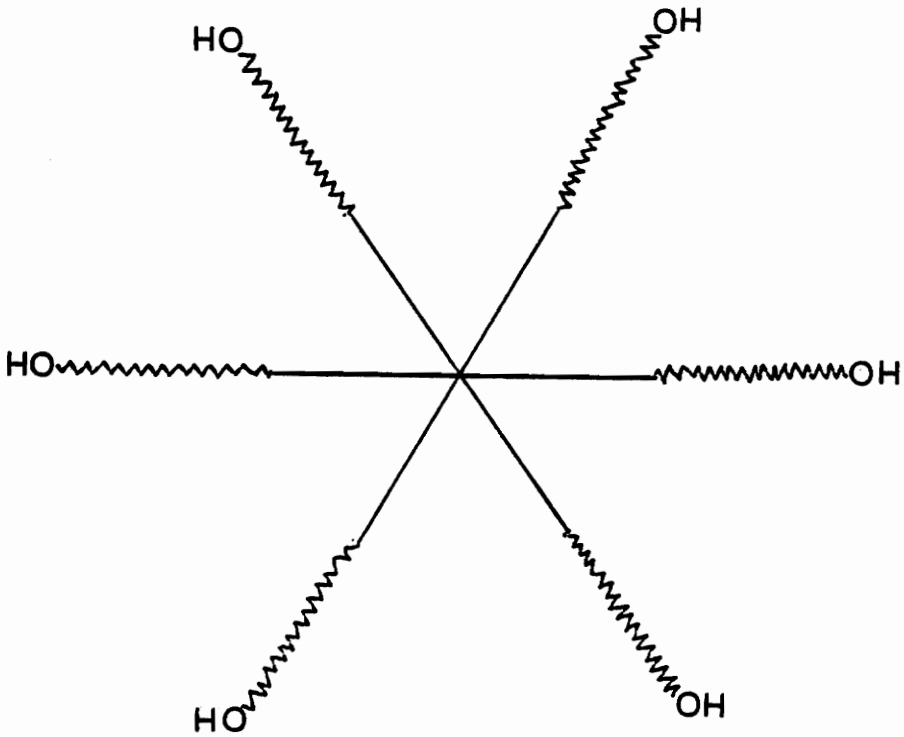

Figure 1. Schematic representation of a 6-point radial HPL star-like structure.

schematically in Figure 2. The choice of $DESO_4$ was dictated by the convenience of synthesis and quantitative analysis. Since the HPL structure generally does not contain ethoxyl groups, their quantitative determination (such as by a modified Zeisel technique and gas chromatographic separation of alkyliodide (29)) allows the establishment of the degree of capping. Other options available for capping the HPL hydroxyl groups are dimethylsulfate, or a monoisocyanate, such as n-butyl isocyanate (11).

The CEHPL is to be prepared following a method developed by Kelley and Nieh (25, 44). It consists of reacting HPL with propylene oxide under non-aqueous conditions using KOH as a catalyst in combination with a phase transfer agent, as shown schematically in Figure 3. The degree of chain-extension with propylene oxide will be determined by the arm length of the star-like macromer.

2.4 Methods of Analysis

2.4.1 Hydriodic Acid/Gas Chromatography

Hodges et al. (29) developed a technique for the determination of molar substitution levels in cellulose ethers containing methoxyl, ethoxyl, hydroxyethyl, and hydroxypropyl groups. A catalyst, such as adipic acid, is used to allow the Zeisel cleavage reaction to proceed quantitatively and without the formation of ethylene and propylene, as is observed in other methods (29). An *in-situ* extraction of the resulting alkyliodides with o-xylene allows for the gas chromatographic

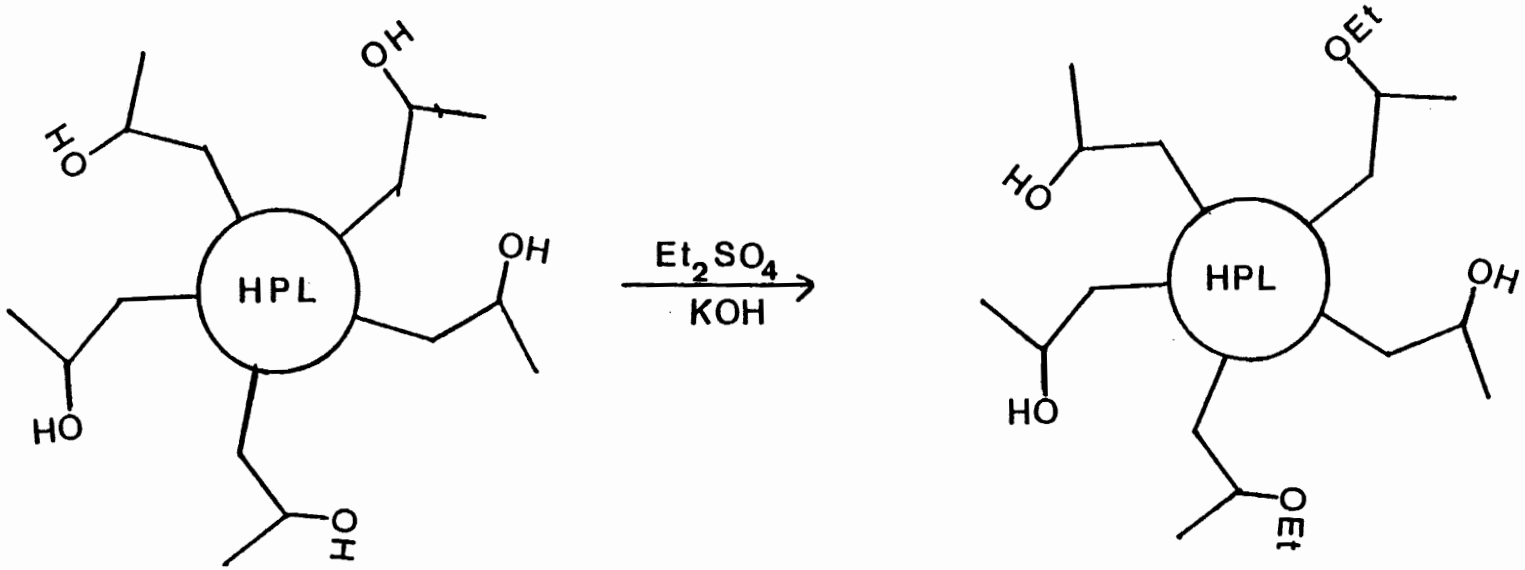

Figure 2. Schematic representation of a capping reaction.

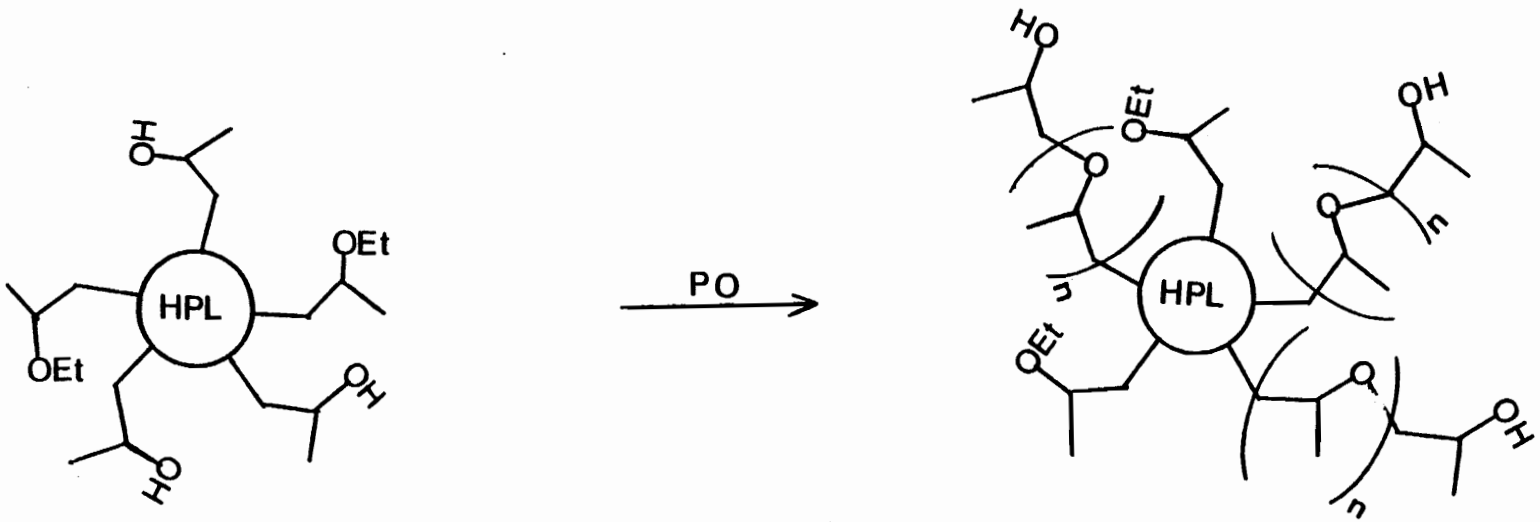

Figure 3. Schematic representation of a HPL chain extension reaction with PO.

determination of substituents in mixed or homogeneous cellulosic ethers.

The applicability of this method is directly dependent on the quantitative conversion of the substituted alkoxyl unit to the corresponding iodide by reaction with hydriodic acid.

The reactions taking place may be illustrated by

$$R\text{–}O\text{–}CH_3 + HI \xrightarrow{cat.} RI + CH_3I \qquad \text{(Eq. 2.1)}$$

$$R\text{–}O\text{–}CH_2CH_3 + HI \xrightarrow{cat.} RI + CH_3CH_2I \qquad \text{(Eq. 2.2)}$$

$$R\text{–}O\text{–}\left[\begin{array}{l} CH_2 - \overset{\overset{O\text{———}H}{|}}{CH} - CH_3 \end{array}\right]_n + HI \xrightarrow{cat.} RI + {}_nCH_3\text{–}\overset{\overset{I}{|}}{CH}\text{–}CH_3 \qquad \text{(Eq. 2.3)}$$

These reactions are acid catalyzed, and quantitative conversion is achieved by using organic acids such as adipic, succinic, formic, acetic, citric or valeric acid (29).

Without the presence of xylene, it was observed that the quantitative formation of 2-iodopropane can not be achieved due to the effect of a disproportionation reaction. This side reaction occurs when the iodide is not extracted from the hydriodic acid.

$$2C_3H_7I \longrightarrow C_3H_8 + C_3H_6 + I_2 \qquad \text{(Eq. 2.4)}$$

The disproportionation step was confirmed when 2-iodopropane was heated in the presence of hydriodic acid with and without o-xylene being present. Without xylene both propane and propylene appeared in the reaction medium and a loss of 2-iodopropane was noted. With o-xylene, no propane was observed and essentially 100% of the 2-iodopropane was recovered.

Another important aspect observed by Hodges et al. is that the quantitative conversion is somewhat dependent on structure. They reported that model compounds having ethoximer or propoximer contents greater than 2, such as tetraethylene glycol or tetrapropylene glycol, required higher temperatures, more catalyst, and longer reaction times to obtain quantitative recovery. The same was observed with alkoxyl groups substituted on aromatic rings that required more severe conditions.

2.4.2 Ultraviolet Spectroscopy

Different from the polysaccharides of the cell wall which do not absorb visible or ultraviolet light, lignin distinctly absorbs in the ultraviolet region due to its aromatic character. The ultraviolet spectra of different lignins are usually quite similar no matter how the lignin was prepared (31).

Figure 4 shows a typical UV spectrum of lignin. It exhibits a maximum at about 200 to 210 nm, a minimum near 260 nm and a lower maximum at about 280 nm followed by a slope towards the visible region of the light spectrum.

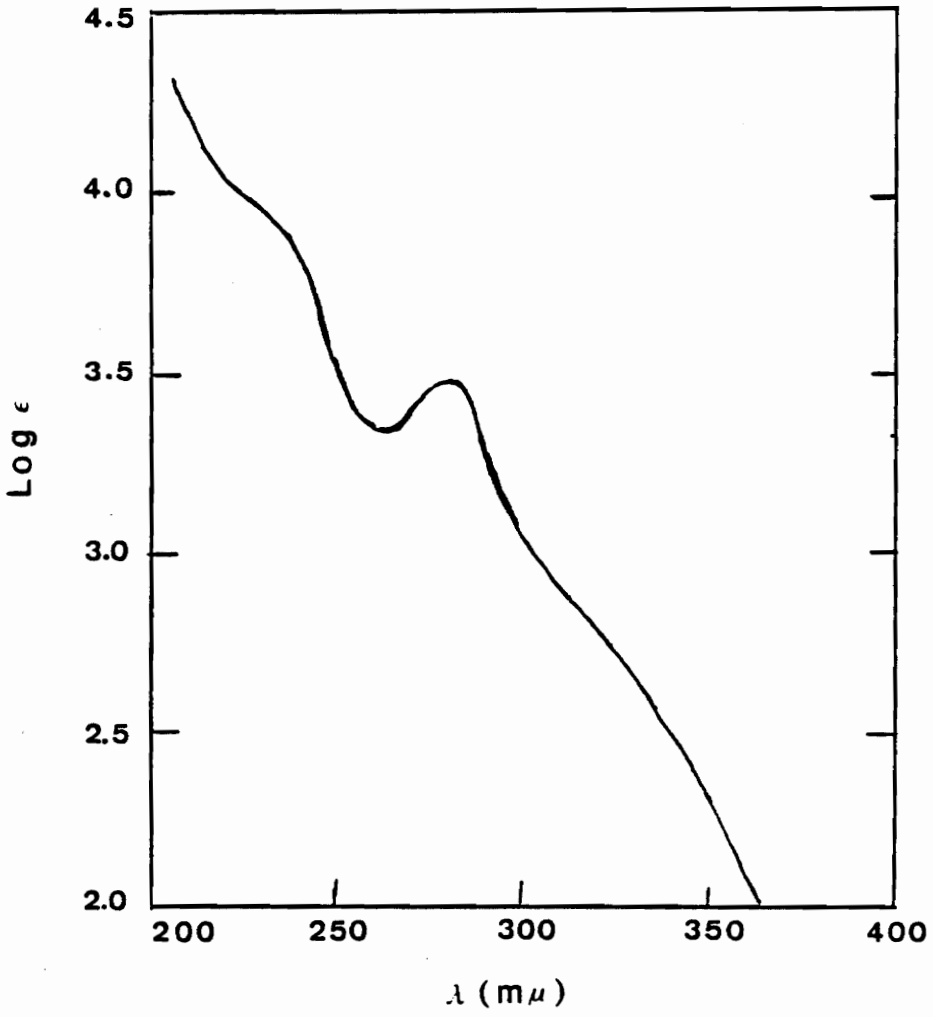

Figure 4. Typical ultraviolet spectra of lignin (31).

The absorption spectrum is a composite of the absorption bands of the different phenylpropane units that constitute the lignin polymer (31). Although there are many conflicting interpretations, these bands are usually attributed to absorption by the free and etherified hydroxyl groups (38). Absorption at 300-350 nm is due to a carbonyl or ethylene double bond in conjugation with the aromatic ring.

The sum of phenylpropane units with several chromophoric structural elements is responsible for the strong absorption of lignin in the ultraviolet range (35). Figure 5 shows various chromophoric groups present in lignin molecules (35). According to Hon and Glasser (39) the main potential chromophoric groups on lignin are:

- Chromophoric functional groups

  phenolic hydroxyl group, double bonds, carbonyl groups, etc.

- Chromophoric systems

  quinone methides, biphenyls, etc.

- Leucochromophoric systems

  methylene quinones, phenanthrene quinones,

  phenylnaphthalenediones, bimethylene quinones, etc.

- Intermediate

  free radicals

- Complexes

  chelate structures with metal ions

Table 1 summarizes absorptivity coefficients of different lignins measured in various solvents at 280 nm. The values demonstrate the generally higher absorptivity coefficient of softwood lignins (19.7 -

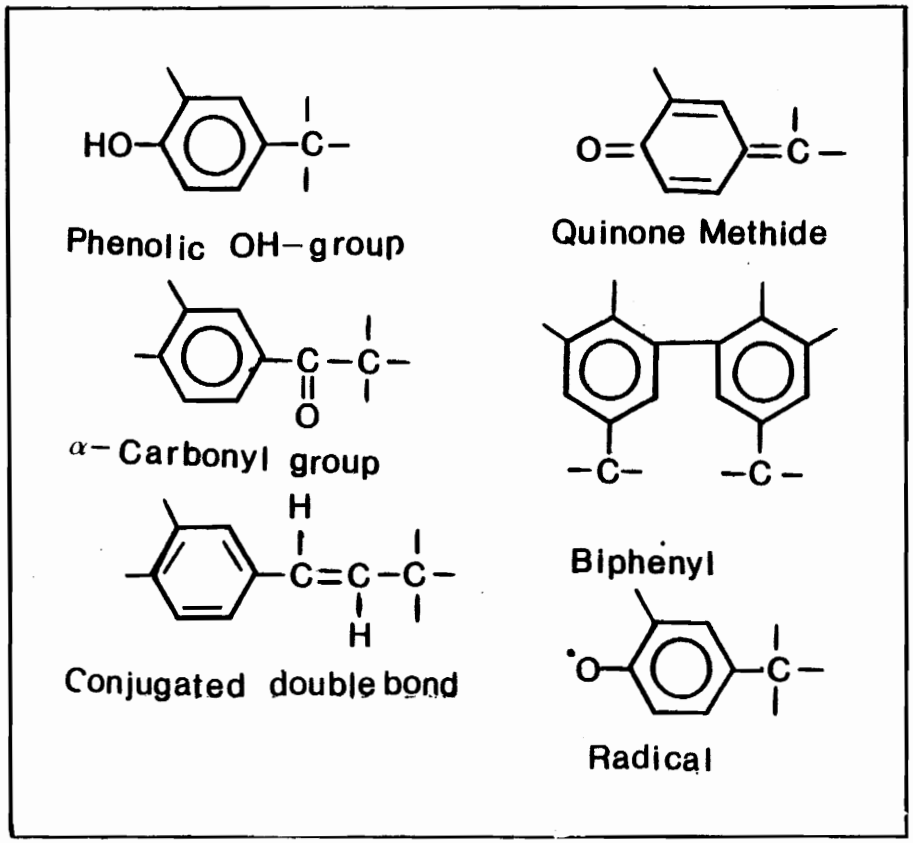

Figure 5. Various chromophoric groups present in lignin molecules (35).

Table 1. Absorptivity Coefficients of Lignins (35)

Lignin	a_{280} Lg^{-1} cm^{-1}	Solvent
MWL spruce	16.7	Methyl cellosolve
MWL spruce	19.0	Alkali/H_2O
MWL spruce	20.7	Formamide
EIL spruce	12.5	Dioxane/H_2O
MWL spruce	19.5	Dioxane
MWL pine	18.8	Methyl cell./ethanol
MWL hemlock	17.7	Methyl cell./ethanol
MWL Douglas fir	19.7	Methyl cell./ethanol
MWL larch	20.2	Methyl cell./ethanol
MWL spruce	19.2	AcBr/acetic acid
MWL beech	13.0	Methyl cellosolve
MWL beech	13.3	Formamide
MWL poplar	14.2	Methyl cell./ethanol
MWL maple	12.9	Methyl cell./ethanol
MWL lauan	17.0	Methyl cell./ethanol/H_2O
Dioxane lignin poplar	12.6	Dioxane
Ethanol/H_2O lignin spruce	25.8	Methyl cellosolve
Lignin sulfonate spruce	11.9	H_2O
Lignin sulfonate beech	10.4	H_2O
Lignin sulfonate softwood	11.9	H_2O
Kraft lignin pine	24.6	H_2O
Kraft lignin pine	26.4	Methyl cell./H_2O

20.7 $Lg^{-1}cm^{-1}$) as compared to hardwood lignins (12.6-14.2 $Lg^{-1}cm^{-1}$) which their maximum of absorption is somewhat shorter wavelengths in the range of 275-277 nm.

Due to lignin's distinct absorption characteristics, ultraviolet spectroscopy has been widely used as a tool for lignin identification, both for qualitative and quantitative determinations and for the characterization of changes in lignin structure and properties (35).

The hydroxypropylation reaction modifies some chemical and physical properties of lignin (9). This chemical modification addresses specifically the phenolic hydroxyl groups and converts them into phenylethers, and it preserves lignin's aromatic character. Since the oxygen-substituted aromatic ring stays unmodified, it is expected that no substantial change will occur in the absorption behavior of these lignin derivatives.

However, with an increasing molar substitution, that is, an increasing number of PO units per arm due the chain-extension reaction, a decrease is expected in the absorptivity coefficient since the nature of the propylene oxide chain is non-UV absorbing.

Bowman and Battaglini (30) in a recent study developed a method that employs ultraviolet analysis for the determination of ethylene-oxide chain length in nonylphenols. The method is based on the absorbance of the para-disubstituted ring of the nonylphenol that is read at the peak maximum around 275 nm. To the extent that the ethylene-oxide chain increases in length, the absorbance becomes less as the aromatic ring content in the sample is diluted by the non-absorbing

material (ethylene-oxide chain). Consequently, absorptivity rather than absorbance measures aromaticity when compared to a previously defined regression line relating absorptivity to hydroxyl value (an indirect measure of extent of ethoxylation).

Based on this property and on the similarity between lignin and the nonylphenols, this UV method was adopted for the determination of the degree of chain extension in star-like macromers from lignin.

2.4.3 H-NMR Spectroscopy

The utility of H-NMR spectroscopy for the structure elucidation of organic substances is well established and has been amply demonstrated for soluble lignins and lignin model compounds by work of Ludwig et al. (40). The H-NMR technique is based on two phenomena: the "chemical shift" and the electron coupled spin-spin interactions between protons. The chemical shift allows the detection of the varying degrees with which bonding electrons interact with externally applied magnetic field; and the spin spin interactions allow observations to be made regarding the interrelationship between protons within the molecule (31). These two phenomena are responsible for a direct quantitative relationship between the intensity of each signal and the number of protons responsible for it.

A currently used way to express H-NMR chemical shift values is the number of parts per million grams (ppm) below (i.e., shifted toward the less shielded values) the original given by tetramethylsilane (TMS). These values are currently referred as delta (δ) values.

Glasser et al. (9) have applied H-NMR spectroscopy as a routine method for the quantitative determination of OH contents in hydroxyalkyl lignins. The method is based on the pioneering studies of Ludwig et al. for characterizing lignin by H-NMR. As a lignin derivative, the hydroxypropyl lignin contains a multitude of protons connected with carbon and oxygen atoms that can give signals with widely varying values in the NMR spectrum. Despite its good solubility, the acetylation of HPL has proved to be more convenient for NMR analysis since the acetoxy groups exhibit a distinct and quantitative signal in the spectrum.

A typical H-NMR spectrum of an acetylated HPL is shown in Figure 6. Due to its complexity it is more convenient to divide the spectrum into ranges to determine the percentages of total signal strength found within selected ranges of δ -values. These ranges represent aromatic protons (range 2), a multitude of aliphatic carbon-linked protons (range 3), CH_2 and methoxyl protons (range 4), aromatic acetoxy protons (range 6), aliphatic acetoxy protons (range 7), and methyl protons (range 8).

The number of protons estimated per C_9 unit in range 7 is of particular interest because it allows the computation of the number of aliphatic acetoxyl (and by inference, hydroxyl groups in the parent preparations). Another peculiarity of this spectrum concerns the nature of the peak in range 8. This distinct and well-resolved peak originates from the methyl protons of the propylene oxide substituent, and it can be used for obtaining quantitative information on the number of PO units in the HPL. Since three protons are equivalent to one PO unit, the

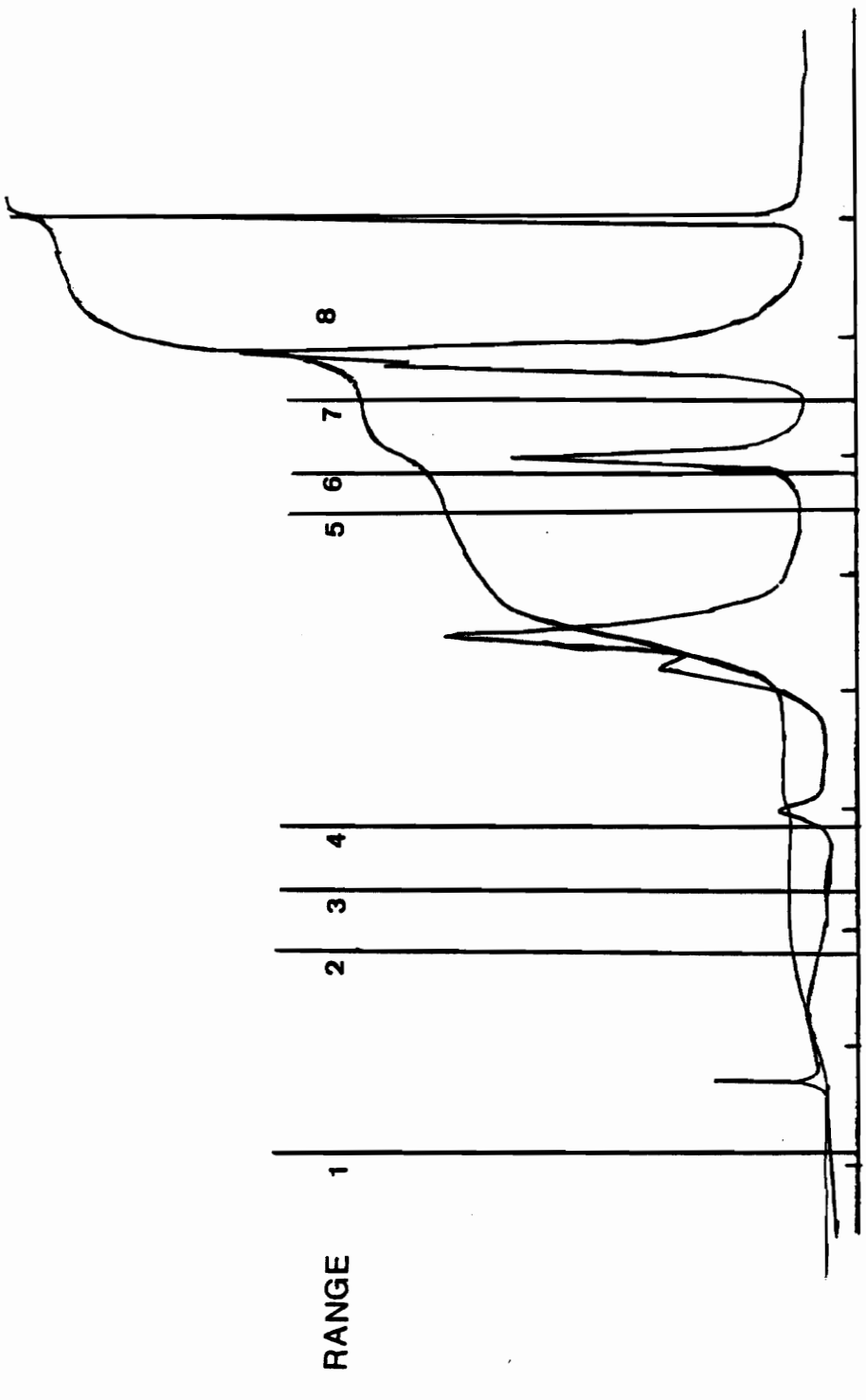

Figure 6. Typical H-NMR spectrum for acetylated HPL with assignment by range.

ratio between range 8 and 7 provides information on the average number of propoxy units linked chain-like to each other in the copolymer.

From a structural point of view, the only difference between HPL and the chain-extended HPL is the number of PO units linked to each other per arm. As this information can be given by the methyl signals in range 8, it is likely that the H-NMR technique can be used to successfully determine arm length in chain-extended HPL.

However, for the capped HPL (with diethylsulfate), it seems that this technique has some limitations.

In the synthesis of the star-like macromer, the number of arms is controlled by partial capping of hydroxyl groups. The agent for that in these experiments is diethylsulfate. The ethoxyl group incorporated into the HPL molecule by this reaction has the same highly shielded protons, according to Ludwig et al., as the propoxyl groups which yield a signal in range 8. Both ethoxyl and propoxyl groups have protons attached to a carbon which has at least two carbons between it and any oxygen function ($H-CH_2CH_2O-$) that consequently can generate a source of highly shielded proton signals.

Thus, it seems difficult to distinguish the two types of protons for a highly capped HPL and its respective chain extended parent, since they produce signal in the same range. Consequently, it appears to be possible to determine only the average arm length of the copolymer in those samples which were uncapped.

2.4.4 Thermal Analysis

The dynamic mechanical properties of materials are determined when they are deformed under periodic stress. The most basic of all mechanical properties are the dynamic modulus and internal friction. The former indicates stiffness of polymeric materials under the dynamic stress and strain condition, and the latter, also called dynamic loss modulus, mechanical damping, or $\tan \delta$, is sensitive to many kinds of molecular motion, transitions, relaxation processes, structural heterogeneities, and the morphology of multiphase systems (crystalline polymers, polymer blends, and copolymers).

The study of the dynamic modulus and damping factor over a wide range of temperatures and frequencies is extremely useful for the recognition of polymer structures and for variations of properties in relation to their performances. Based on these dynamic parameters, it is possible to determine the glass transition temperature region, relaxation properties, degree of crystallinity, etc.

Generally, the dynamic mechanical properties of polymers are studied over a wide temperature range (-150 to +300^{o}C). Typical dynamic mechanical properties of polymers as a function of temperature are illustrated in Figure 7.

The glass transition appears when the dynamic modulus E changes abruptly from approximately 1 GPa (10^{10} dyne/cm^2) in the glassy state to about 1 MPa (10^{7} dyne/cm^2) in the rubbery state. Other relaxations may be found in the glassy state, below the temperature of the primary dispersion. These are called secondary dispersions and they are usually

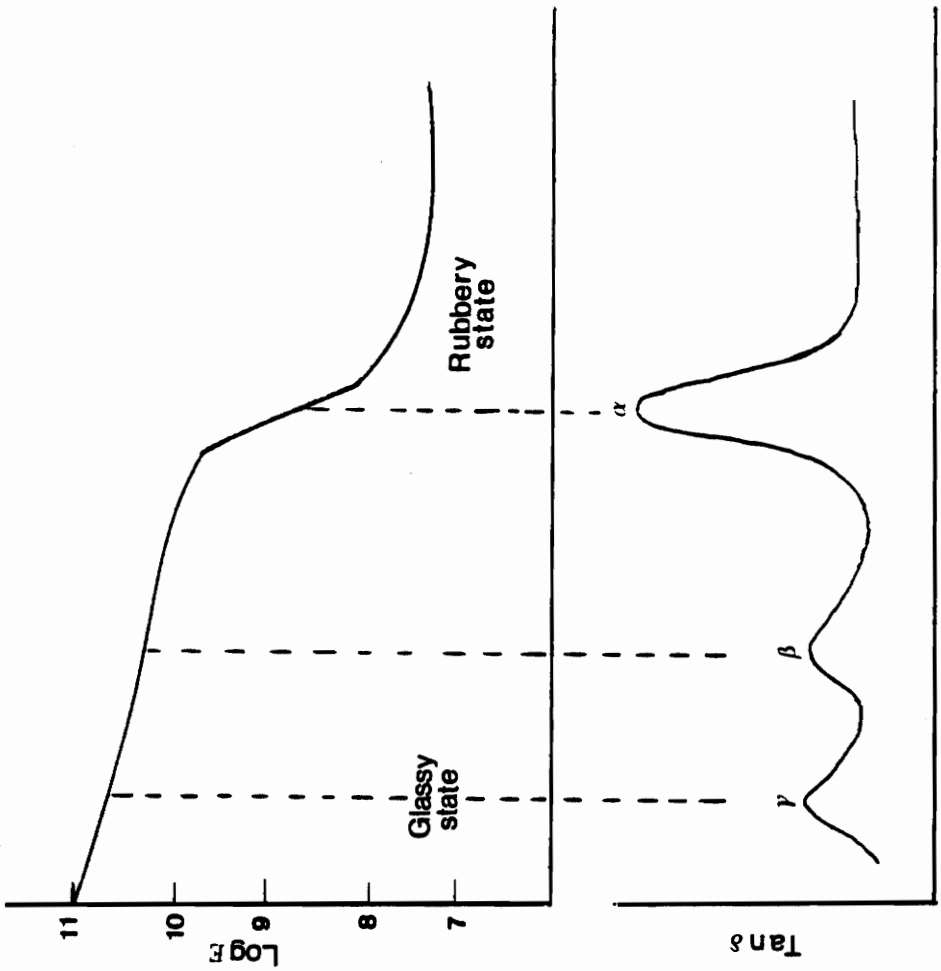

Figure 7. Typical dynamic mechanical properties of polymers (41).

designated as β, γ, etc., transitions in order of decreasing temperature (41).

Effect of Copolymerization on Tg

The glass transition temperatures of copolymers can vary linearly or nonlinearly with composition. As a first approximation it is reasonable to expect that the glass transition of the copolymer will be intermediate between the glass transition of the corresponding homopolymers. In fact, this is true for random copolymers for which the T_g can be calculated from the Gordon-Taylor equation (42),

$$T_g = \frac{Kw_2Tg_2 + w_1Tg_1}{w_1 + Kw_2} \qquad \text{(Eq. 2.5)}$$

where w_1 and w_2 are the weight fraction of the macromer residues 1 and 2, T_g is the transition temperature for the copolymer in degrees Kelvin, and Tg_1 and Tg_2 are the transitions for the two homopolymers. Constant K is given by

$$K = (\alpha_{L,2} - \alpha_{g,2})/(\alpha_{L,1} - \alpha_{g,1}) \qquad \text{(Eq. 2.6)}$$

where $\alpha_{L,1}$, $\alpha_{L,2}$, $\alpha_{g,1}$ and $\alpha_{g,2}$ are the coefficients of cubical expansion of the 1 and 2 polymers in the liquid (rubbery) and in the glassy states.

In the case of block and graft copolymers the above considerations cannot be applied since a separate T_g will be observed for each

component polymer. However, when the blocks and branches are not long enough to permit each homopolymer type to segregate into its own region, the Gordon-Taylor equation can be used successfully (43).

Lignin is a material of poor solubility in organic solvents, and it has a high glass transition temperature (165-185°C) (35). However, the hydroxypropylation of lignin can reduce the T_g by around 50-75°C below the glass transition temperature of their parent lignin depending on the nature of the starting material. This can either be explained by disruption of hydrogen bonds of phenolic hydroxyl groups or by increased free volume (9).

Glasser et al. (45) have studied the effect of several alkylene oxides on T_g, and the T_g was found to decline as result of the increase in the number of alkylene oxide substituents in the HPL. The glass transition behavior of CEHPL was found to follow the Gordon-Taylor relationship for copolymers.

Thus, thermal analysis will be applied in this study not as a method for the determination of CEHPL composition, but as an indication, according to T_g values, of an increase in chain extension.

Among the dynamic methods for measuring T_g are DSC and DMTA. However, DSC is not adequate for HPL and derivatives since it often generates transitions which are too subtle to detect. A more appropriate technique is based on DMTA. This technique detects all motional transitions in the polymer and usually provides the most sensitive means of studying T_g.

Since HPL and its derivatives are low modulus materials, they will be blended with incompatible (thermoplastic) polymers, which produce samples with adequate stiffness, and which generate two distinct glass transitions.

III. OBJECTIVES

The objective of this study is to synthesize star-like macromers from lignin, and to explore quantitative methods of analysis describing macromer architecture. The specific goals of the study are:

(1) To synthesize a series of capped HPL derivatives for the preparation of star-like macromers with variable number of arms. The average number of arms per macromer will be controlled by partial capping of the hydroxyl groups with diethylsulfate; and the average length of arms will be controlled by the degree of chain-extension with propylene oxide.

(2) To analyze the HPL and CEHPL products by total hydroxyl group determination, vapor pressure osmometry, hydriodic acid/gas chromatography, ultraviolet spectroscopy, H-NMR spectroscopy, and thermal analysis.

(3) To develop a quantitative method for the determination of the degree of capping and chain-extension.

IV. MATERIALS AND METHODS

4.1 Materials

4.1.1 Organosolv Lignins.

Organosolv lignin was supplied by the Biological Energy Corporation, Valley Forge, Pennsylvania, and this was isolated from aspen wood chips with aqueous ethanol in a pilot plant digester (44).

4.1.2 Hydroxypropyl Lignin.

The HPL was synthesized from the organosolv lignin by reaction with propylene oxide in toluene at 180°C, using KOH as catalyst. A typical HPL synthesis consisted of reacting 30 g of lignin, 1 g KOH, 40 mL propylene oxide and 120ml toluene in a 300 mL stainless steel mechanically stirred (Parr, Inc.) reactor. The reactor was sealed, heated externally, and stirred vigorously. The final product was a tarry mixture of poly (propylene oxide) and hydroxypropyl lignin. The individual components contained in this mixture were then separated by extraction with n-hexane from acetonitrile solution in a liquid-liquid extractor, followed by precipitation into water of pH 4. The isolated and purified HPL was a solid yellow powder with good solubility characteristics (25).

4.1.3 Lignin Model Compounds.

The hydroxypropyl and acetylated hydroxypropyl model compounds were obtained in the lab as described elsewhere (9). The other compounds were all commercially available and they were used as received.

4.2 Methods

4.2.1 Synthesis and Purification

4.2.1(a) Capping Reaction with Diethyl-Sulfate

Aliphatic OH groups of HPL were partially capped with diethylsulfate in aqueous KOH, at room temperature. The ethylation consisted of dissolving 100g of HPL in 500 mL of acetone in a three-necked round bottom flask. Potassium hydroxide (25-50g) was added to maintain an alkaline medium (pH 12) throughout the reaction. A variable amount of diethylsulfate was then added dropwise into the solution, and the reaction was kept going overnight under a constant flow of N_2. At the end of the reaction, the pH was adjusted to 2.0-3.5 with 5N HCl, the mixture was heated to destroy any remaining diethylsulfate, and the product was extracted from the solution with chloroform in a separatory funnel. After extraction and drying (Na_2SO_4) the solution was freed from chloroform by evaporation under reduced pressure (rotation evaporation). The resulting syrup was precipitated into a large excess (ca:10:1) of acidified H_2O. The precipitate was filtered, washed and freeze-dried.

4.2.1(b) Chain Extension Reaction

The chain extension reaction with propylene oxide and HPL was performed in a 300 mL Parr reactor equipped with a heating mantle, mechanical stirrer, pressure gauge, cooling loop, safety valve, and thermocouple. A typical reaction mixture consisted of 10.0 g of HPL (0.03 moles), 1.87 g of KOH (0.03 moles), 187 g of a phase transfer agent (quaternary ammonium salt) (0.005 moles) and 150 mL of toluene (1.63 moles). A volume of 5.0 mL of propylene oxide was added to the reaction mixture, the reactor was sealed and heated to 80^{o}C. After the PO had been consumed as was indicated by the drop of pressure (3 to 0 atm) in the reactor, another batch of 5.0 mL PO was then added and the reaction proceeded in the same way. The total amount of PO per reaction was established to be 27 and 34 mL PO per gram of sample (1.5 and 3.0 g PO/g HPL). It was expected that this method produced two different levels of chain extension.

4.2.1(c) Isolation of CEHPL

The reaction product was isolated by evaporation of solvent and dissolution in acetonitrile. Liquid-liquid extraction with n-hexane/acetonitrile was used to remove propylene glycol, oligomers and homopolymers also formed during the reaction. The acetonitrile-soluble fraction was evaporated, redissolved in methanol, and dialyzed for the removal of the catalyst.

4.2.1(d) Molecular Weight Determination

Molecular weights of HPL and some CEHPL were determined by vapor pressure osmometry (VPO). The VPO apparatus was calibrated with benzil (46).

4.2.2 Analysis of CEHPL

4.2.2(a) Hydriodic Acid/Gas Chromatography

A modified Zeisel technique, combined with gas chromatographic separation of alkyliodides was applied in this study for the evaluation of the degree of capping by ethoxyl groups and the degree of chain extension by propylene oxide (29).

Procedure

An internal standard solution containing 3.48 mg 1-iodopropane/ml o-xylene was prepared by diluting with o-xylene 100 microliters of 1-iodopropane into a 50 mL volumetric flask.

Dry HPL (20-30 mg) was weighed into a 5 mL microreaction vessel. An amount of adipic acid approximately equal to the sample weight was added. Internal standard stock solution (2 mL) was pipetted into the microreaction vessel, and 0.75 mL of HI was added. The microvessel was immediately capped with the Mininert valve top and weighed before insertion into the hot heating block. Samples were reacted for 1 hr. at around 140^{o}C with frequent shaking.

After 1 hr. the microreaction vessel was removed from the heating block, cooled and reweighed to determine any loss due to leakage.

Factors

Relative response factors were used to generate factors for subsequent use in the internal standard calculations. They were generated by the following procedure:

10 μL of iodomethane, iodoethane, 1-iodopropane and 2-iodopropane were diluted with xylene in a 10 mL volumetric flask. 0.5 μL of this standard solution were injected into the gas chromatograph and the relative response factors were determined by programming the integrator.

The percent of alkoxyl was calculated by the following equations:

$$OCH_3(\%) = \frac{mgCH_3I\ (factor)}{wt\ Sample\ (mg)} \times \frac{OCH_3\ (mol.\ wt)}{CH_3I\ (mol.\ wt)} \times 10^3 \quad \text{(Eq. 4.1)}$$

$$OC_2H_5 = \frac{mgC_2H_5I(factor)}{wt\ Sample\ (mg)} \times \frac{OC_2H_5(mol.\ wt)}{C_2H_5I(mol.\ wt)} \times 10^3 \quad \text{(Eq. 4.2)}$$

$$OC_3H_7(\%) = \frac{mgC_3H_7I(factor)}{wt\ Sample\ (mg)} \times \frac{OC_3H_7(mol.\ wt)}{C_3H_7I(mol.\ wt)} \times 10^3 \quad \text{(Eq. 4.3)}$$

Apparatus

A Varian 3700 gas chromatograph equipped with a flame ionization detector and a 9 ft chromosorb column packed with 10% SP1000 and 1% H_3PO_4-100-120 were used. The oven temperature was 45°C; the injection port and detector temperatures were 210°C, and N_2 was the carrier gas at a pressure of 20 psi.

A CDS 111L data system interfaced with the Varian 3700 was used to provide fully automated chromatographic date processing and control. A micro reaction vessel, capped with Mininert valves to contain the Zeisel

cleavage reaction products, and a multi-block heater to control the temperature were used (29).

4.2.2(b) Ultraviolet Spectroscopy.

Procedure

To determine the absorptivity coefficent of the model compounds, a sample having an accurately known weight between 0.9 and 4.0 mg was dissolved in methanol and diluted to a known volume. The solution was scanned in the ultraviolet region from 250 to 320 nm and analyzed for the absorbance at the band maximum and at 280 nm. The absorptivity then was calculated and plotted as a function of known non-UV absorbing mass represented either by the extent of propoxylation or propoxylation-acetylation. A straight line was drawn from the starting model (SM) absorptivity to the respective propoxylated model (PO), and from the latter to the acetylated model (PO-Ac). Their respective slopes were calculated. In the case of vanillyl alcohol, the acetylation doubled the non-UV absorbing mass, due to the two OH of the compound.

For lignin, HPL and CEHPL, a sample having a weight between 20.0-25.0 mg was dissolved in methanol and diluted to a known volume. The absorbance of the solution was then analyzed at 280 nm.

The absorptivity coefficient of the samples was determined on a VARIAN/CARY-219 UV-VIS spectrophotometer.

4.2.2(c) H-NMR Spectroscopy

Procedure

The H-NMR spectra were obtained from HPL and CEHPL on a Brucker 270 MHz instrument using deuterochloroform as a solvent and TMS as an internal standard.

The H-NMR spectrum was divided in to six distinct regions of chemical shifts (ranges) for the quantitative assessment of the distributions of hydrogen in the macromer. These regions according to Glasser et al. (9) represent range 2 (aromatic protons (4.5-5.7 δ)), range 3 (aliphatic carbon-linked protons (4.5-5.7 δ)), ranges 4 and 5 (CH_2 and methoxy protons (2.5-4.5 δ)), range 7 (aromatic acetoxy protons (1.6-2.5 δ)), and range 8 (carbon-linked methyl protons (0.9-1.6 δ)).

The degree of chain extension was determined by taking the ratio between range 8 and range 7 proton signals from the spectrum integration.

For the capped HPL's and their CEHPL's the calculation of the degree of chain extension was not straightforward, since both ethoxyl and propoxyl groups generate highly shielded proton signals in range 8. Thus, a factor to discount the proton signals due to ethoxyl groups was used. A second factor taking in to account the degree of capping in the calculation of the degree of chain extension was also considered. Both factors are discussed in section 5.3.

4.2.2(d) Thermal Analysis

Procedure

Glass transition temperatures were determined by dynamic mechanical thermal analysis (DMTA) using an instrument from Polymer Laboratories Ltd., England. It is a microprocessor-based instrument capable of determining the damping factor ($\tan\delta$) and dynamic modulus (E) of polymeric materials.

Polyblends were prepared by blending 20-40% of HPL or CEHPL with (60-80%) of one of the polymers listed in Table 2 by injection into a dogbone mold of a Mini Max Molder of Custom Scientific Instruments, N.J. The extrusion temperature varied from 160°C to 190°C.

The dogbones were analyzed in the DMTA instrument over the temperature range of -100°C to +100°C at a rate of 4°C per minute. Frequency was 10 Hz and strain factor was x4. Both the dynamic storage modulus and the damping factor were recorded as functions of temperatures.

4.2.2(e) Titration of Total OH Content

The total hydroxyl content of HPL and capped HPL was determined by acetylation and back titration of free acetic acid (28) using a BRINKMANN E576 Potentiograph.

100 mg of dry sample (HPL or capped HPL) and 15 mg of vanillyl alcohol were weighed into a 5 mL micro reaction vessel. An amount of 0.5 mL of dimethyl-formamide (DMF) was added to dissolve the solids. 400 mg of the pyridine-acetic anhydride reagent 3:0.9 volume was

Table 2. Polymers Used for Blends

Polymers	Composition	Supplier	Cat. #	Lot #	T_g(°C)
Ethylene/ vinyl acetate (ETPVA 18)	18% vinyl acetate	Scientific Polymer Products, Inc.	244	4	-12
Polyethylene low density (PE)	-	Scientific Polymer Products, Inc.	042	9	-120
PMMA	-	Polysciences, Inc.	4552	44488	105

pipetted to the micro reaction vessel, and the vessel immediately capped with the Mininert valve top. Samples were reacted overnight at 50°C on a heated block. The micro reaction vessel was rinsed with acetone into a beaker following an addition of 100 mL of water. The beaker was covered with parafilm and let stand for 1 hour. The titration was performed on a BRINKMANN titrator using 0.1N KOH (standardized).

Calculation

$$\% \text{ OH} = \frac{[(\frac{t}{w} \times w_s) - t_s] \text{ (N KOH)}(0.017)(100)}{\text{Sample wt in grams}} \qquad \text{(Eq. 4.4)}$$

t = mL KOH for blank

t_s = mL KOH for sample

w = mg pyridine/acetic anhydride in blank

w_s = mg pyridine/acetic anhydride in sample

V. RESULTS

5.1 Hydriodic Acid/Gas Chromatography.

5.1.1 Degree of Capping.

A series of capping reactions with variable amounts of diethylsulfate was performed on HPL. The ethoxyl contents of the resulting derivatives were calculated based on equation 4.2. The results are shown in Table 3.

Ethoxyl contents varied between 0.7 and 14.8%. Except for samples 4 and 6, which yielded tarry, highly viscous liquids, all products were solid brown powders. The tarry samples (#4 and 6, Table 3) were obtained using different conditions from the other preparations. These differences involved repeating the ethylation reaction several times. This became necessary because poor phase transfer between KOH and HPL, and thus poor ionization, produced derivatives with ethoxyl contents which remained lower than expected. The samples were therefore resubmitted to the same modification procedure before results approached largest values.

Since it is difficult to dry to solvent-free state, and to weigh with accuracy viscous materials, the ethoxyl content of samples #4 and 6 was determined by extrapolation of the relationship between ethoxyl content and EtI/MeI molar ratio. The absolute amount of alkyliodides was less reliable and significant than their relative ratios.

Table 3. Ethoxyl Content of Capped HPL According to the HI/GC Technique

Sample Number	$DESO_4$ [1] (mM/meq OH)	MeI [2] (mMol $\times 10^{-2}$)	EtI [2] (mMol $\times 10^{-2}$)	i-PrI [2] (mMol $\times 10^{-2}$)	EtI/MeI (molar ratio)	Ethoxyl Content (%)
0	0	5.71	0.27	5.11	0.05	0.73
1	0.56	5.63	1.04	4.92	0.18	3.06
2	0.46	5.65	1.56	4.71	0.28	4.63
3	1.99	4.44	2.31	2.99	0.42	6.70
4[3]	0.93[4]	4.91[5]	2.60[5]	3.67[5]	0.53	7.59[6]
5	0.83	4.58	3.20	2.54	0.70	9.40
6[3]	2.73[4]	5.11[5]	5.49[5]	3.85[5]	1.07	14.77[6]

1) In synthesis mixture using 1.1–3.0 mM KOH/meq OH

2) By GC, per mg of derivative

3) Viscous tar; other samples were solid powders

4) Repeated several times

5) Inconsistent values were attributed to handling difficulties associated with tarry liquids

6) By extrapolation of relationship between ethoxyl content and EtI/MeI ratio

The relationship between the ethoxyl content and the ratio between ethyliodide and methyliodide is shown in Figure 8. The data reflects a strong and linear relationship ($r = 0.99$) between ethoxyl content and EtI/MeI molar ratio. The ethoxyl content of the viscous products was then computed from equation 5.1,

$$\text{Ethoxyl (\%)} = 0.54 + 13.3\ [\text{EtI}]/[\text{MeI}] \qquad \text{(Eq. 5.1)}$$

whose [EtI] and [MeI] are ethyl and methyliodide in molar equivalents.

It was observed that for the degree of capping no rigorous quantitative relationship existed between diethyl sulfate concentration in the synthesis mixture and ethoxyl content of the product. One possible explanation for this variability is that the extremely high alkalinity required for the ionization of the secondary aliphatic OH groups profoundly affected the degree of reaction stoichiometry.

In addition, trace quantities of ethoxyl groups were detected in unethylated HPL (0.73%). This may be due to the introduction of ethoxyl groups during the isolation of lignin with ethanol by organosolv pulping (31) according to the reaction scheme shown in Figure 9. A corrected "true" ethoxyl content can be calculated as demonstrated in Table 4.

The total hydroxyl content of unethylated HPL was 8.33% by potentiometric titration. Considering that the number-average molecular weight (M_n) of HPL was 1200 (46), it was possible to assign an average of 6 hydroxyl groups to each molecule of HPL. Since each OH group can generate a protruding arm, it can be concluded that the uncapped HPL

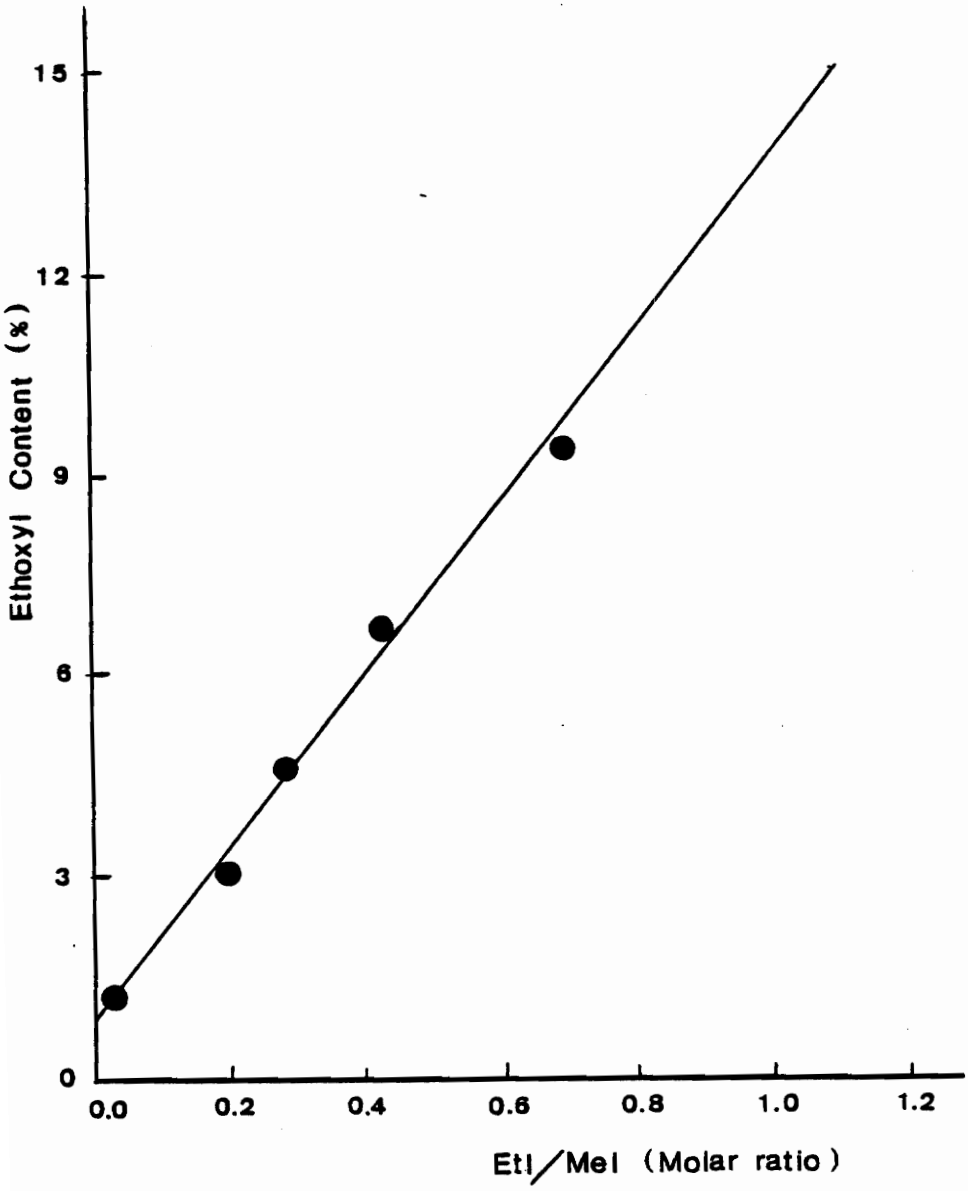

Figure 8. Relationship between ethoxyl content and EtI/MeI (molar ratio).

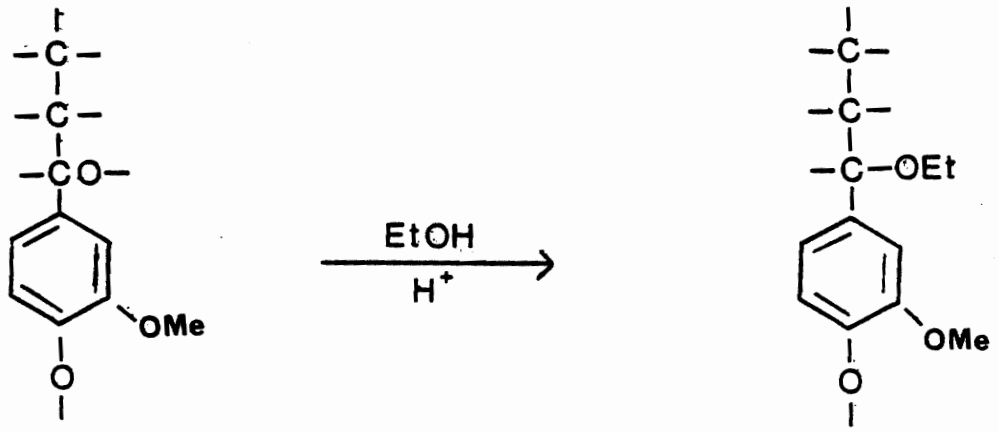

Figure 9. Reaction scheme for the introduction of ethoxyl groups in lignin during organosolv with pulping (31).

architecture has a structure of a star-like molecule (14) with an average of 6 arms per macromer.

The hydroxyl content of the capped HPL varied from 7.61 to 4.86%, or on a different basis, from 4.48 to 2.86 meq. OH/g of capped HPL, Table 4. Considering that the difference in milliequivalents of OH between the original ("parent") HPL (4.9) and the resulting capped HPL's (4.48 - 2.86) should be equivalent to the amount of milliequivalents of ethoxyl, then it is possible to compare the hydroxyl contents determined by potentiometric titration with those derived indirectly by gas chromatography. The data shown in Table 4 reveal that the calculated hydroxyl content values (by gas chromatography) are lower than those experimentally determined by potentiometric titration; and the difference between experimental and calculated data increases as the hydroxyl content in the sample decreases. Figure 10 presents a plot relating hydroxyl and ethoxyl content from both experimental and calculated data. It seems that it is difficult to determine the total hydroxyl content of samples with very low OH functionality by titration. Indeed the difficulty of determining OH increases as the hydroxyl content decreases. Titration of small amounts of hydroxyl groups generally requires samples and reagents (vanillyl alcohol, DMF, acetic anhydride) to be kept in very dry condition.

Thus, the degree of capping is better determined according to the calculated hydroxyl content via gas chromatography (i.e. Table 4) than by potentiometric titration. The degree of capping varied from 0 to 64%, according to Table 4, and this means that the derivative samples

Table 4. Ethoxyl Content, Hydroxyl Content, Degree of Capping and Number Average of Arms of the Capped HPL's.

	Ethoxyl Content		Hydroxyl Content			Degree of capping (%)	No. of arms at 1200g M^{-1}
Sample Number	%	(meq/g)[3*]	% (experimental)	Meq/g (experimental)	meq/g[4*] (calculated)		
0	0.73[1*]	0	8.33	4.9	4.9	0	5.9
1	3.06	0.52	7.61	4.48	4.38	11	5.2
2	4.63	0.87	7.34	4.32	4.03	18	4.8
3	6.70	1.33	6.33	3.72	3.57	27	4.3
4	7.59[2*]	1.53	6.19	3.64	3.37	31	4.0
5	9.40	1.93	6.19	3.64	2.97	39	3.6
6	14.77[2*]	3.12	4.86	2.86	1.78	64	2.1

1*) From solvent retained during delignification (i.e. organosolv with aq. ethanol)

2*) Determined on the basis of ethyliodide-to-methyliodide ratio by HI/GC analysis; and this ratio's relationship to ethoxyl content. (Illustrated in Figure 8)

3*) After correction for "native" ethanol content of uncapped organosolv HPL

4*) Difference between original hydroxyl content and ethoxyl content in meq/g. The relationship between OH content and ethoxyl content (Figure 10) revealed that OH determination was variable at low OH contents.

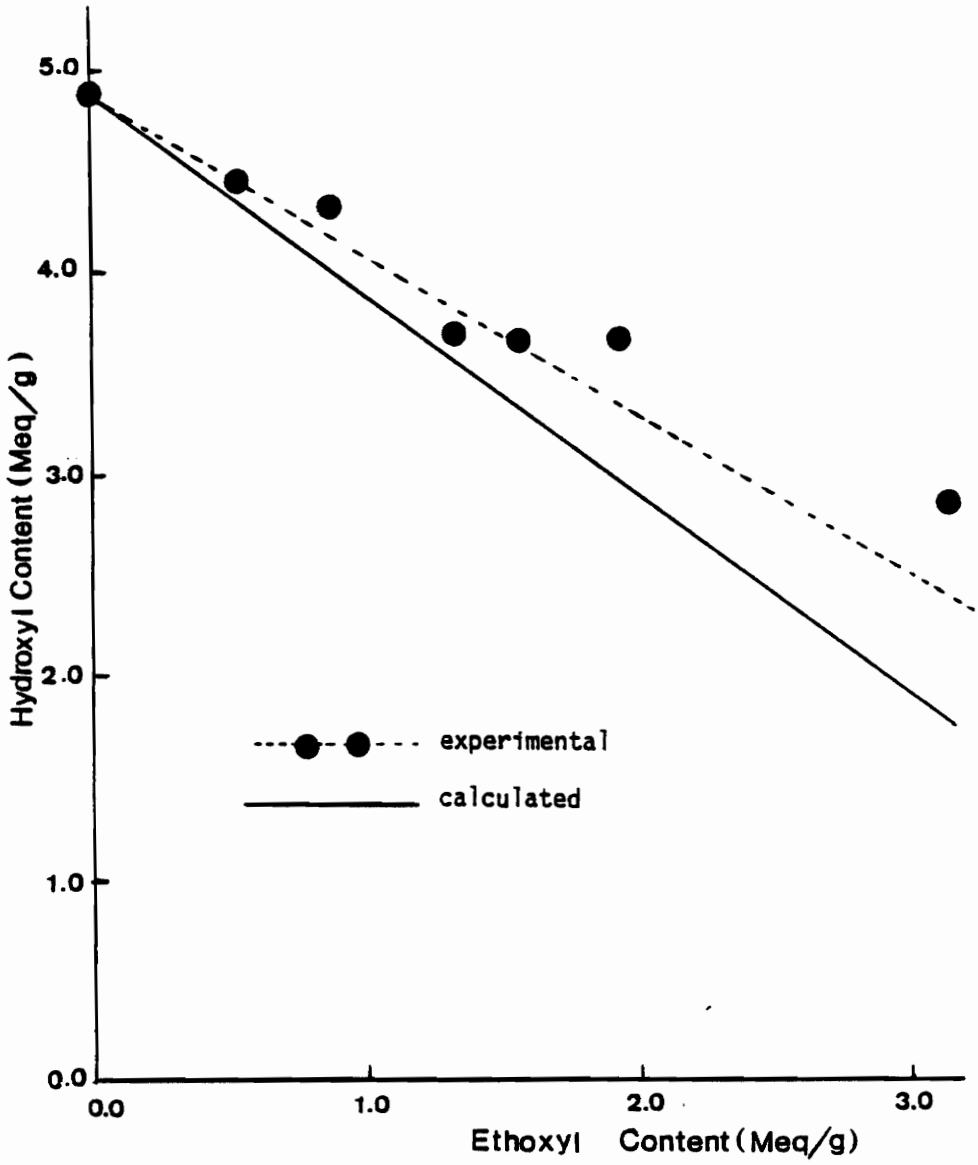

Figure 10. Relationship between hydroxyl and ethoxyl content.

were produced with an average of 6, 5, 4, and 2 hydroxyl groups per macromer.

5.1.2 Chain Extension

The chain extension reaction on HPL and capped HPL was performed with propylene oxide. Since the reactivity of (capped) HPL in relation to propylene oxide is not fully understood, it was decided to react each capped HPL sample with two different but constant amounts of PO. Thus, each sample was reacted with 1.5 and 3.0 g of propylene oxide per gram of capped HPL, or with 25.9 or 51.7 mmol PO/g HPL, respectively. Since each HPL sample had a different hydroxyl content, the amount of PO per OH varied from 5.3 to 28.4 mmol PO per milliequivalent of OH.

Table 5 summarizes synthesis parameters and analysis results according to the gas chromatographic method of a series of chain extension experiments. The alkyliodide species of interest to chain extension was isopropyliodide, just as ethyliodide had been the species of interest to capping. Since the true propoxyl content of each sample depends on the quantitative conversion of the substituted alkoxyl groups to their corresponding alkyliodes (which is not certain for CEHPL), the molar ratio between isopropyl and methyliodide was again taken to be the most sensitive figure for the determination of chain extension. In this way, assuming that the formation of MeI and i-PrI is proportional to their respective concentration in CEHPL, the molar ratio of i-PrI/MeI should be constant regardless of extent of capping.

Table 5. Synthesis Parameters and HI/GC Analysis Results of a Series of CEHPL.

Sample No.	Degree of capping, %	PO/OH Ratio in reaction (mM/meq)			i-Propyliodide / Methyliodide			Ratio (M/M)			i-PrI/MeI / $OH_{eq/g}$			Number average PO units per arm		
		Initial	1.Rct[1]	2.Rct[2]	Initial	1.Rct[1]	2.Rct[2]	Initial	1.Rct[1]	2.Rct[2]	Initial	1.Rct	2.Rct	Initial	1.Rct	2.Rct
0	0	0	5.3	10.6	0.89	2.21	3.43				0.18	0.45	0.70	1.0	2.5	3.9
1	11	0	5.9	11.8	0.87	2.14	3.46				0.20	0.50	0.80	1.0	2.5	4.0
3	27	0	7.2	14.5	0.55	1.66	2.16				0.15	0.46	0.61	1.0	3.0	3.9
4	31	0	7.7	15.4	0.76	1.93	2.48				0.23	0.57	0.74	1.0	2.5	3.3
5	39	0	8.7	17.4	0.55	1.46	2.21				0.19	0.49	0.74	1.0	2.7	4.0
6	64	0	14.3	28.6	0.75	1.21	1.25				0.42	0.68	0.70	1.0	1.6	1.7
mean											0.23	0.525	0.715	1.0	2.5	3.5
Std dev.,%											8.9	7.9	5.8			

1) Reacted with 1.5 g PO/g lignin derivative

2) Reacted with 3.0 g PO/g lignin derivative

As seen in Table 5, the initial i-PrI/MeI ratio varied little, but the two reactions produced significant and consistent changes. For each capped HPL, the higher the amount of PO in the reaction, the higher was the degree of chain extension as indicated by an increase in i-PrI/MeI ratio. Thus, the degree of chain extension, or the number-average propylene oxide units linked to each other, could be calculated by taking the I-PrI/MeI ratio of the chain extended samples and dividing it by its corresponding value prior to chain extension. Based on this, it can be concluded that star-like macromers were obtained with arm lengths averaging 2.5 PO units/arm on those samples reacted with 1.5 g PO/g HPL and 3.5 PO units/arm on samples reacted with 3.0 g PO/g HPL.

This relationship is better illustrated when the (i-PrI/MeI)/OH ratio is plotted versus the degree of capping. This is shown in Figure 11. The three groups of data (0, 1.5 and 3.0 g PO/g HPL) produce slopes of 3.2×10^{-3}, 3.2×10^{-3} and -4.4×10^{-4}, with r^2 values of 0.6, 0.7 and 0.0 respectively. Thus, the data shows that the degree of chain extension is independent of the degree of capping.

This constitutes an important observation since it suggests that the degree of chain extension is independent of PO/OH stoichiometry. As seen, for instance at the first level of propoxylation (i.e. 1.5 g PO/g HPL), the PO/OH ratio varied from 5.3 to 19.3 mmol PO/meq OH (see Table 5), and the resulting CEHPL had an average degree of chain extension of 2.5 PO units/arm ($\pm$20%) regardless of degree of capping. This means that the PO conversion efficiency (i.e. the efficiency of incorporating PO into CEHPL) declines with declining OH content. This implies that

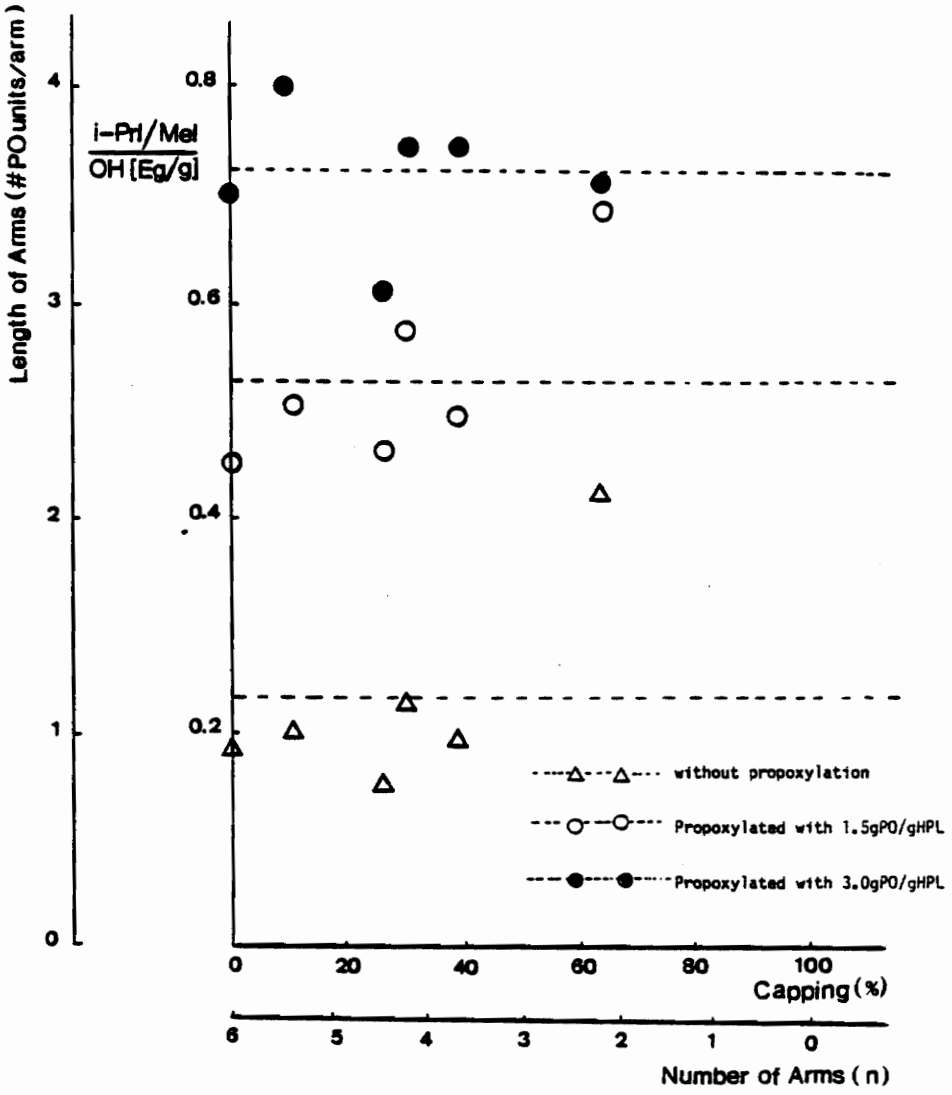

Figure 11. Relationship between (i-PrI/MeI)/OH versus degree of capping (or length of arms x number of arms).

more homopolymer (polypropylene oxide) is formed as the amount of PO per OH equivalent increases in the reaction medium. This statement is limited to constant PO feed rate and catalyst content.

5.2 Ultraviolet Spectroscopy

5.2.1 Lignin Model Compounds

In order to verify whether the UV method by Bowman and Battaglini for analyzing aromaticity of nonylphenols could be applied to propoxylated lignin derivatives, several lignin model compounds were tested regarding their absorptivity versus aromaticity relationship.

Table 6 shows ultraviolet absorption characteristics of a number of lignin model compounds. It is seen that λ_{max} as well as absorptivity, a_{max}, varied among the models. Although some models presented absorption maxima near 280 nm, their absorptivities, on the other hand, showed values that varied from 9.94 to 76.01 (Lg^{-1} cm^{-1}). Nevertheless, propoxylation was observed to consistently produce reductions in absorptivity, similarly to nonylphenols (30).

Due to the wide range of absorptivities and absorption maxima (i.e. wavelengths), it was impossible to develop an equation that related a_{max} to aromaticity. This indicates that the ultraviolet analysis procedure is highly substrate-specific, and that the method can only be applied to separate substances.

The ultraviolet spectra of the model compounds also showed that guaiacol and vanillyl alcohol represent lignin better, and are better

Table 6. Ultraviolet Spectra of Lignin Model Compounds

No.	Compound	max (nm)	a_{max} (Lg^{-1} cm^{-1})	min (nm)	a_{min} (Lg^{-1} cm^{-1})	max (nm)	a_{max} (Lg^{-1} cm^{-1})	MW
I	Guaiacol	276	21.9	246	2.1			124
1	Guaiacol-PO	274	12.3	246	0.5			182
2	Guaiacol-PO-Ac	275	11.0	246	0.6			224
II	2,6-Dimethoxyphenol	268	10.2	250	4.2			154
3	2,6-Dimethoxyphenol-PO	268	3.3	248	1.3			212
4	2,6-Dimethoxyphenol-PO-Ac	266	2.9	248	1.0			254
III	Vanillin	278	58.3	246	18.5			152
5	Vanillin-PO	274	55.2	244	8.3			210
6	Vanillin PO-Ac	274	38.9	244	14.4			252
IV	Vanillic acid	252	58.1	274	20.4	284	24.3	168
7	Vanillic acid-PO	248	48.2	270	13.5	284	18.1	226
7Ac	Vanillic acid-PO-Ac	248	39.4	270	15.0	284	15.0	268
V	Ferulic acid	286	83.0	254	30.5			194
8	Ferulic acid-PO	284	56.5	252	18.8			252
9	Ferulic acid-PO-Ac	284	53.3	252	18.8			294
VI	Syringic acid	262	49.6	234	15.8			198
28	Syringic acid-PO	252	35.6	230	13.7			256
29	Syringic acid-PO-Ac	252	31.7	230	12.7			298
VII	Vanillyl Alcohol	280	19.3	250	3.2			154
5R	Vanillyl Alcohol-PO	278	12.4	250	1.8			212
6R	Reduced Vanillin--PO-Ac	278	9.9	251	1.7			296
VIII	Isoeugenol	258	67.3	238	40.1			164
16	Isoeugenol-PO	258	66.6	236	31.1			222
17	Isoeugenol-PO-Ac	256	52.0	236	28.3			264
IX	Eugenol	280	76.0	252	6.6			164
18	Eugenol-PO	280	13.0	250	3.0			222
19	Eugenol-PO-Ac	278	12.9	248	5.4			264

lignin-like models than other models, since they do not have C=C or C=O groups conjugated with the aromatic ring. This is probably the reason why guaiacol and vanillyl alcohol have absorptivities near 20 Lg^{-1} cm^{-1}, which is a lignin characteristic when the absorbance is read at 280 nm (31). Although there are different interpretations for explaining this phenomenon (32), the presence of C=O and C=C group conjugated with a benzene ring generally shifts the absorption maximum to a shorter wavelength. This is seen in models IV, VI, VIII and their respective derivatives.

Like lignin, guaiacol and vanillyl alcohol have absorption maxima near 280 nm; but unlike lignin, the absorption curves drop abruptly to 0 at 300 nm and to nearly 0 at 250 nm before rising again and thereby forming a deep trough as shown by the λ_{min} values and the spectra.

Tables 7 and 8 give the absorptivity and slope values of the set of models for both a_{max} and 280 nm data. These slopes show that besides the absorptivity diversity, there was no consistency with regard to the ratio of Δ a/non-UV absorbing mass. This suggests again that each set of models has its own characteristic spectral features, and for this reason cannot be averaged.

In order to verify the possibility of calculating non-UV absorbing mass via absorptivity coefficient of the original model, some calculations for the "predicted" a_{max} were performed. Table 9 compares both observed and calculated absorptivity coefficients for the models and their respective derivatives. Although the non-UV absorbing mass on the model compounds studied was restricted to only one PO unit or to one

Table 7. Absorptivity and Slopes for λ_{max}

No	State of Compound	Absorptivity ($Lg^{-1}cm^{-1}$)	Non-UV absorbing$^{-1*)}$ mass (NUVAM) ($gmol^{-1}$)	$\Delta a_{(\Delta NUVAM^{2*})}$ (SM–PO)	$\Delta a(\Delta NUVAM^{3*})$ (PO–POA_c)
I	oil	21.9			
1	oil	12.3	58	0.166	
2	cryst	11.0	100		0.031
II	cryst	10.2	0		
3	oil	3.3	58	0.119	
4	oil	2.8	100		0.012
III	cryst	58.3	0		
5	cryst	55.2	58	0.053	
7	cryst	38.9	100		0.388
IV	cryst	58.1	0		
6	cryst	48.2	58	0.171	
7Ac	cryst	39.4	100		0.210
V	cryst	83.0	0		
8	cryst	56.5	58	0.457	
9	cryst	53.3	100		0.076
VI	cryst	49.6	0		
28	cryst	35.6	58	0.241	
29	cryst	31.7	100		0.093
VII	cryst	19.3	0		
5R	oil	12.4	58	0.119	
6R	oil	9.9	192		0.030
VIII	oil	67.3	0		
16	cryst	66.6	58	0.012	
17	oil	52.0	100		0.398
IX	oil	76.0	0		
18	oil	13.0	58	1.086	
19	oil	12.9	100	0.002	

1*) Non-Uv absorbing mass added to the starting model compound during derivatization (i.e., propoxylation and/or acetylation).

2*) Ratio between the decrease in absorptivity coefficient due to derivatization and the increase of NUVAM of the starting and derivatized model.

3*) Ratio between the decrease in absorptivity coefficient due to derivatization and the increase of NUVAM of the propoxylated and propoxylated–acetylated model.

Table 8. Absorptivity and Slopes for $\lambda = 280$

No	State of Compound	Absorptivity ($Lg^{-1}cm^{-1}$)	Non-UV absorbing mass (NUVAM) ($gmol^{-1}$)	$\Delta a_{(\Delta NUVAM^{2*})}$ (SM–PO)	$\Delta a(\Delta NUVAM^{3*})$ (PO–POA_c)
I	oil	19.8	0		
1	oil	9.3	58	0.181	
2	cryst	8.7	100		0.014
II	cryst	6.0	0		
3	oil	0.9	58	0.088	
4	oil	1.0	100		-0.002
III	cryst	56.9	0		
5	cryst	50.6	58	0.109	
6	cryst	35.9	100		0.350
IV	cryst	22.0	0		
7	cryst	17.3	58	0.081	
7Ac	cryst	14.2	100		0.074
V	cryst	78.1	0		
8	cryst	55.2	58	0.395	
9	cryst	52.9	100		0.055
VI	cryst	25.4	0		
28	cryst	7.3	58	0.312	
29	cryst	7.4	100		-0.002
VII	cryst	19.3	0		
5R	oil	12.3	58	0.121	
6R	oil	9.9	142		0.029
VII	oil	31.5	0		
16	cryst	23.3	58	0.191	
17	oil	18.9	100		0.105
IX	oil	76.0	0		
18	oil	13.0	58	1.086	
19	oil	12.4	100	0.014	

1*) Non-Uv absorbing mass added to the starting model compound during derivatization (i.e., propoxylation and/or acetylation).

2*) Ratio between the decrease in absorptivity coefficient due to derivatization and the increase of NUVAM of the starting and derivatized model.

3*) Ratio between the decrease in absorptivity coefficient due to derivatization and the increase of NUVAM of the propoxylated and propoxylated-acetylated model.

Table 9. Observed and Calculated Absorptivity Coefficient for Model Compounds and Derivatives

Compound Number (s. Table 6)	MW ($g\ mol^{-1}$)	λ_{max} (nm)	a_{max} ($Lg^{-1}\ cm^{-1}$) (Observed)	a_{max} ($Lg^{-1}\ cm^{-1}$) (calculated)[1*)]	State
I	124	276	21.9		oil
1	182	274	12.3	14.9	oil
2	224	275	11.0	12.1	cryst
II	154	268	10.2		cryst
3	212	268	3.3	7.4	oil
4	254	266	2.8	5.9	oil
III	152	278	58.3		cryst
5	210	274	55.2	42.2	oil
6	252	274	38.9	35.2	oil
IV	168	252	58.1		cryst
7	226	248	48.2	43.2	cryst
7Ac	268	248	39.4	36.4	cryst
V	194	286	83.0		cryst
8	252	284	56.5	63.9	cryst
9	294	284	53.3	54.8	cryst
VI	198	262	49.6		cryst
28	256	252	35.6	38.4	cryst
29	298	252	31.7	33.0	cryst
VII	154	280	193		cryst
5R	212	278	12.4	14.0	oil
6R	296	278	9.9	10.0	oil
VIII	164	258	67.3		oil
16	222	258	66.6	49.7	cryst
17	264	256	52.0	41.9	oil
IX	164	280	76.0		oil
18	222	280	13.0	56.1	oil
19	264	278	12.9	47.2	oil

1*) Based on the assumption that an increase in non-uvabsorbing mass results in a proportional decrease in absorptivity coefficient.

acetylated propylene oxide segment, in general, there was significant agreement between the observed and calculated a_{max}. In fact, for those "true" lignin-like models guaiacol and vanillyl alcohol, and also for syringic acid, the calculated absorptivities were very similar to the experimental values. The small remaining difference may be more the result of inaccuracies in determining the exact weight of the oily materials than one of shortcomings of the method.

Polymeric hydroxypropyl lignin, which displays surprisingly little variation in λ_{max} and a_{max} values, can probably be analyzed more successfully by UV spectrometry regarding PO content than can model compounds.

Conclusions Regarding UV-Spectroscopy of Model Compounds:

1. The UV absorptivity lignin models decreases as a result of propoxylation.

2. The UV analysis procedure for PO determination is highly substrate-specific, and the method can only be applied to individual models.

3. As polymeric HPL has relatively constant a_{max} values for a given λ_{max}, the UV method holds promise for propylene-oxide chain length determination.

5.2.2 HPL and CEHPL

The study with lignin-like model compounds revealed that the absorptivity coefficient decreases with the incorporation of non-UV

absorbing mass. This may result from either propylene oxide or acetate groups. It was also observed that for some models, such as guaiacol, vanillyl alcohol and syringic acid, the calculated absorptivity coefficient, based on the addition of nonabsorbing mass, was very similar to the experimental values.

If polymeric HPL and its PO chain-extended derivatives were to exhibit this property of decreasing absorptivity with increasing amount of non-absorbing mass, the ultraviolet analysis method could become a useful tool for measuring the extent of propoxylation and chain extension.

Table 10 summarizes the absorptivity coefficient at 280 nm for organosolv (ethanol) lignin, its respective HPL and several CEHPL derivatives. All the extended samples presented lower absorptivity coefficients than the parent HPL. This can be interpreted as a signal of "dilution" in concentrations of UV_{280}-absorbing groups in HPL or, in other words, an increase in the propylene oxide chain length. The (parent) lignin had the highest absorptivity coefficient among all samples, and the HPL and capped HPL's (excepting those with 7.6 and 14.8% of ethoxyl content-samples #4 and 6) displayed an almost constant absorptivity value. (Again, the probable reason for the low absorptivity achieved in the 7.6 and 14.8% ethoxy samples is attributed to the difficulty of obtaining exact weights of tars and viscous materials.)

Figure 12 gives a plot of UV absorptivity coefficient versus i-PrI/MeI molar ratio. Although the curve has only 3 points, a

Table 10. UV Absorptivity Coefficient (280nm) and i-PrI/MeI (Molar Ratio) of Organsolv (ethanol) Lignin, HPL and CEHPL Derivatives.

Sample Number[1*)]	Absorptivity (a_{280}) Coefficient (Lg^{-1} cm^{-1})	i-PrI/MeI (molar ratio)
Organosolv (ethanol) lignin	27.4	-
0	22.1	0.9
0-I[2*)]	15.3	2.2
0-II[3*)]	12.1	3.4
1	22.4	0.9
1-I	17.0	2.1
1-II	13.5	3.5
2	21.5	0.8
3	21.4	0.6
3-I	17.6	1.7
3-II	15.5	2.2
4	16.2	0.8
4-I	16.0	1.9
4-II	14.1	2.5
5	21.0	0.6
5-I	18.9	1.5
5-II	16.3	2.2
6	9.7	0.8
6-I	14.7	1.2
6-II	15.6	1.3

1*) See Table 5

2*) Chain extended at the first level of propoxylation (1.5 g PO/g HPL)

3*) Chain extended at the second level of propoxylation (3.0 g PO/g HPL)

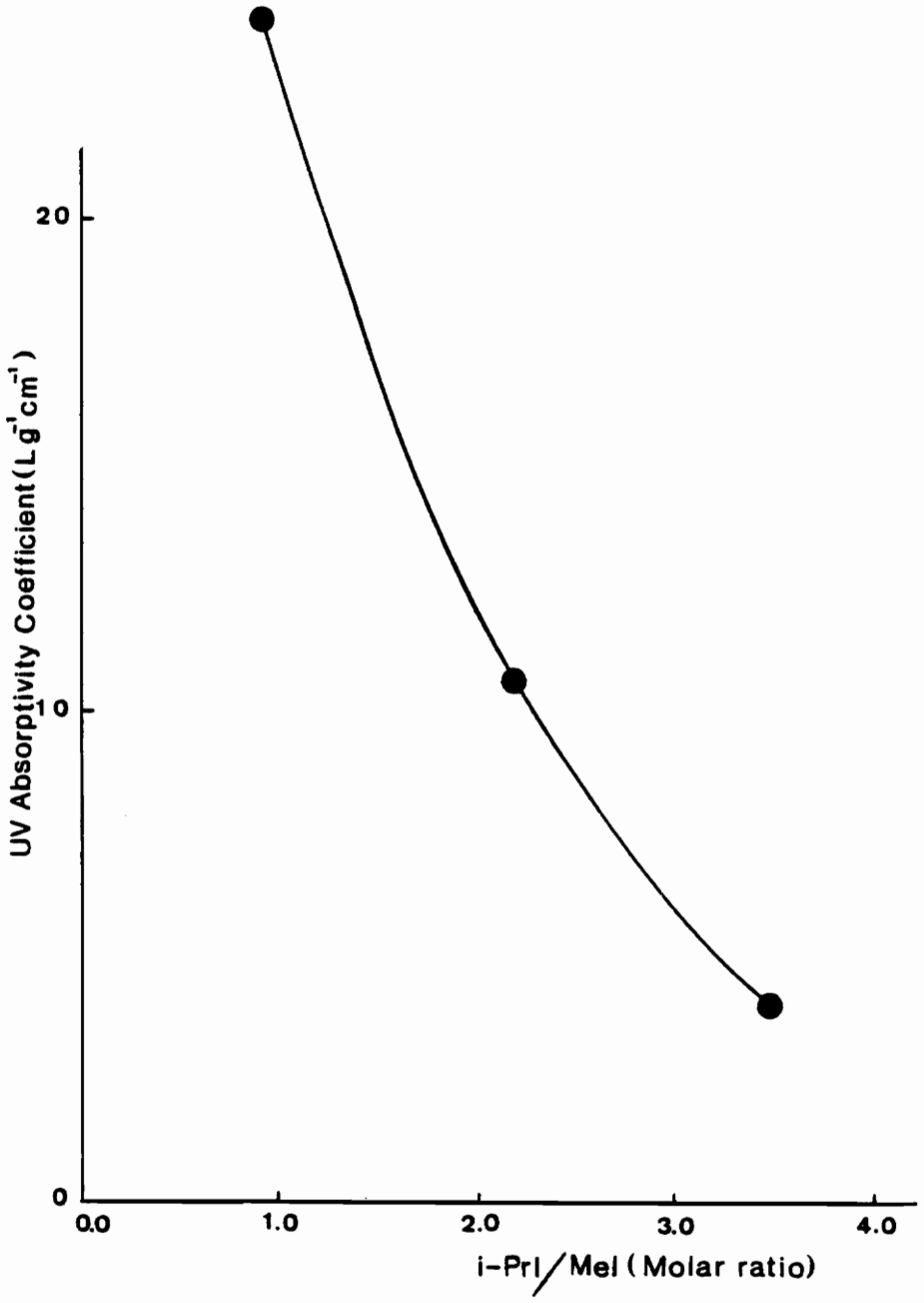

Figure 12. UV-Absorptivity coefficient (280 nm) versus i-PrI/MeI (molar ratio) for uncapped HPL and chain extended derivatives.

consistent decrease in the absorptivity coefficient is revealed as result of the chain extension on the star-like macromer. Since the absorptivity coefficient also changes with degree of capping, each series of chain extended samples generates a different curve.

In terms of non-UV absorbing mass a general decrease in absorptivity coefficient was observed as result of capping and/or chain extension. Table 11 shows the HPL derivative compositions (based on ethoxyl and propoxyl content) and their respective absorptivity coefficients at 280 nm. The total non-UV absorbing mass versus the absorptivity coefficient were plotted on Figure 13. (This ignores the viscous samples with 7.6 and 14.8% ethoxyl content-samples 4 and 6-and then CEHPL-I and II derivatives). A significant linear relationship (r^2 = 0.923) between absorptivity and non-UV absorbing mass is detected. Since most of the CEHPL non-UV absorbing mass (91-99%) originates from the propoxylation and is linearly related to the absorptivity coefficient, it can be concluded that UV spectrometry can be applied for the determination of the propylene-oxide chain length.

The absorptivity coefficients of HPL and CEHPL samples are plotted versus ethoxyl content in Figure 14. The 3 groups of data (i.e. 0, 1.5 and 3.0 g PO/g HPL) produced straight line relationships with slopes of -0.15, 0.38 and 0.50 with r^2 values of 0.81, 0.94 and 0.98, respectively. It seems that linear relationships exist between UV-absorptivity coefficient and ethoxyl content for each individual group. For the uncapped HPL series, the absorptivity coefficient decreases slowly as the degree of capping increases. The reverse is

Table 11. UV-Absorptivity Coefficient (280 nm) and Non-UV Absorbing Mass of HPL and CEHPL Derivatives.

Sample Number	OC_2H_5 (%)	OC_3H_7 (%)	Total non-UV absorbing mass g/Kg HPL	a_{280} (Lg^{-1} cm^{-1})
0	0.73	18.25	189.8	22.1
0-I[1*)]	0.39	30.37	307.6	15.3
0-II[2*)]	0.41	38.29	387.0	12.1
1	3.06	18.98	220.4	22.4
1-I	0.45	29.90	303.5	17.0
1-II	0.22	40.34	405.6	13.5
3	6.70	11.41	181.1	21.4
3-I	3.82	26.24	300.6	17.6
3-II	3.26	29.66	329.2	15.5
4	7.61	14.11	217.2	16.2
4-I	3.05	27.47	305.2	16.0
4-II	2.65	31.63	342.8	14.1
5	9.45	9.84	192.9	21.0
5-I	3.43	21.87	253.0	18.9
5-II	2.95	29.83	327.8	16.3
6	14.8	17.61	322.1	9.7
6-I	3.88	16.18	200.6	14.7
6-II	3.92	17.89	218.1	15.6

1*) Chain extended at the first level of propoxylation (1.5 g PO/g HPL)

2*) Chain extended at the second level of propoxylation (3.0 g PO/g HPL)

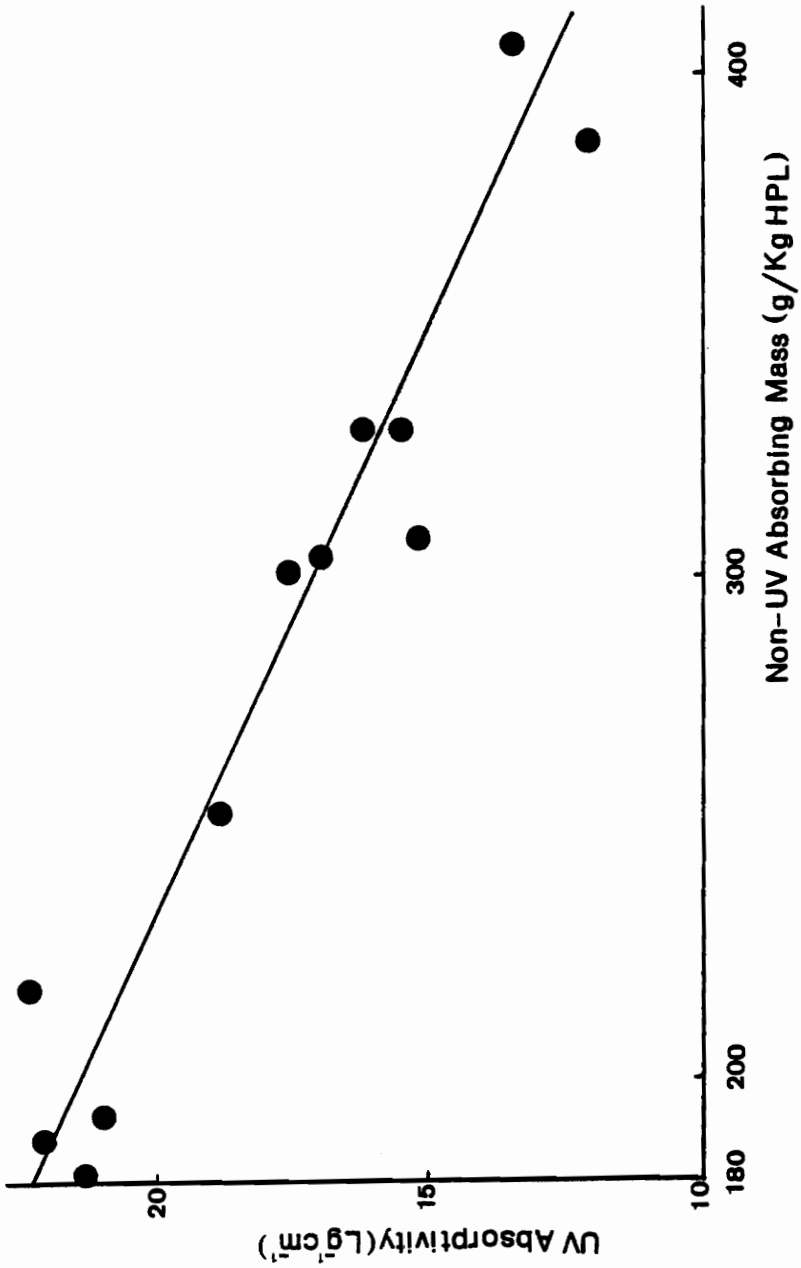

Figure 13. UV-Absorptivity coefficient (280 nm) versus non-UV absorbing mass in CEHPL.

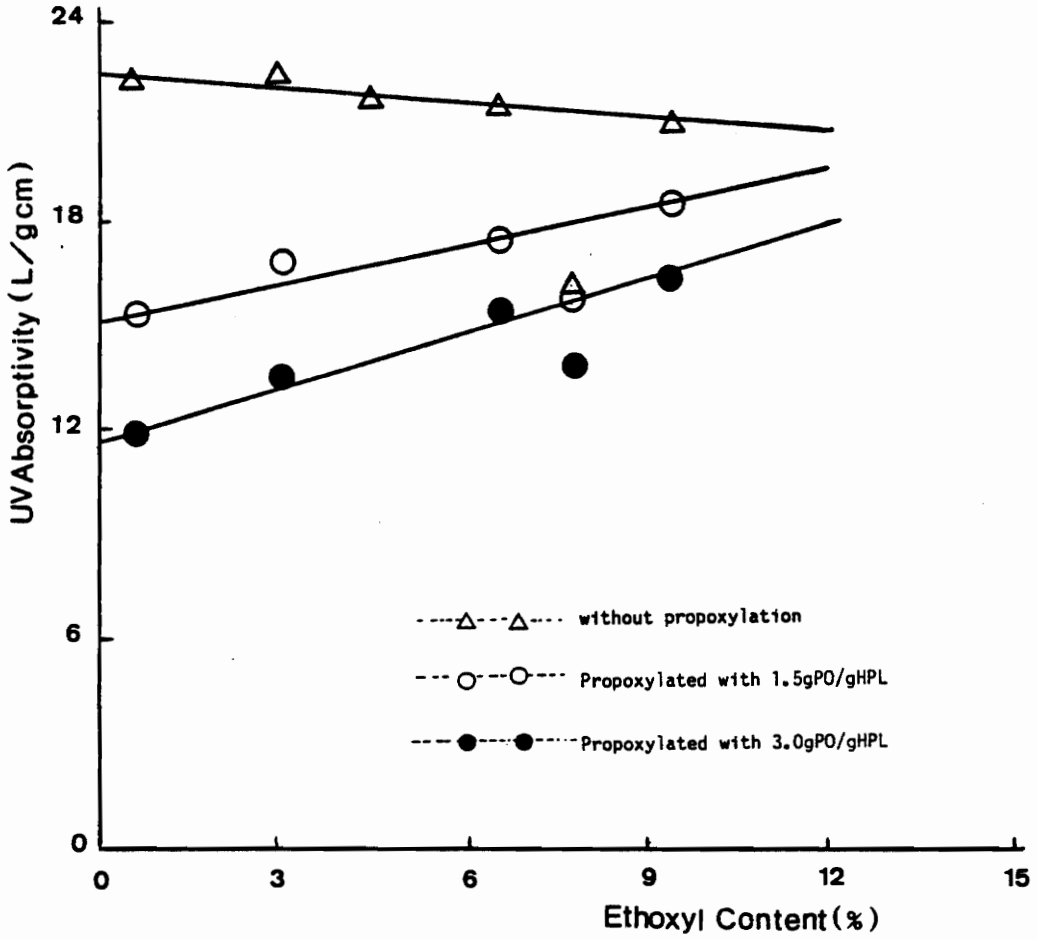

Figure 14. Relationship between uv-absorptivity and ethoxyl content for CEHPL.

true for CEHPL: the absorptivity coefficient increases with the degree of capping.

The absorptivity coefficient of (parent) lignin of 27.4 Lg^{-1} cm^{-1} far exceeds those of all HPL derivatives. The precipitous decline of a_{280} when lignin is chemically modified with PO cannot be explained by dilution of aromaticity alone, but must be viewed in relation to dramatic changes in chemistry: from a phenol to an aryl-alkyl ether. This change in chemistry seems to overshadow any changes in aromaticity, and it determines absorptivity. Consequently, it appears that the UV method must be confined to determining the extent of chain extension of propoxylated lignin and that it cannot be extended to parent lignin.

5.3 H-NMR Spectroscopy

Figure 15 presents 3 typical H-NMR spectra of acetylated HPL, and CEHPL samples at 2 levels of propoxylation (1.5 and 3.0 g PO/g HPL). The spectra were sectioned in accordance with chemical shifts of proton signals in acetylated HPL (9).

Table 12 gives the results from 19 spectra of HPL's with varying degree of capping and two levels of chain extension. Also presented in this table are the i-PrI/MeI molar ratios from HI/GC. On the whole, it was observed that for chain extended samples, the higher the i-PrI/MeI molar ratio, the higher was the peak responsible for the methyl protons of propylene oxide (i.e. range 8). The capped HPL's lost aliphatic acetoxyl protons (i.e., H-NMR in range 7) as a consequence of the reduction of OH groups (i.e. fewer O-Ac protons). A decrease in

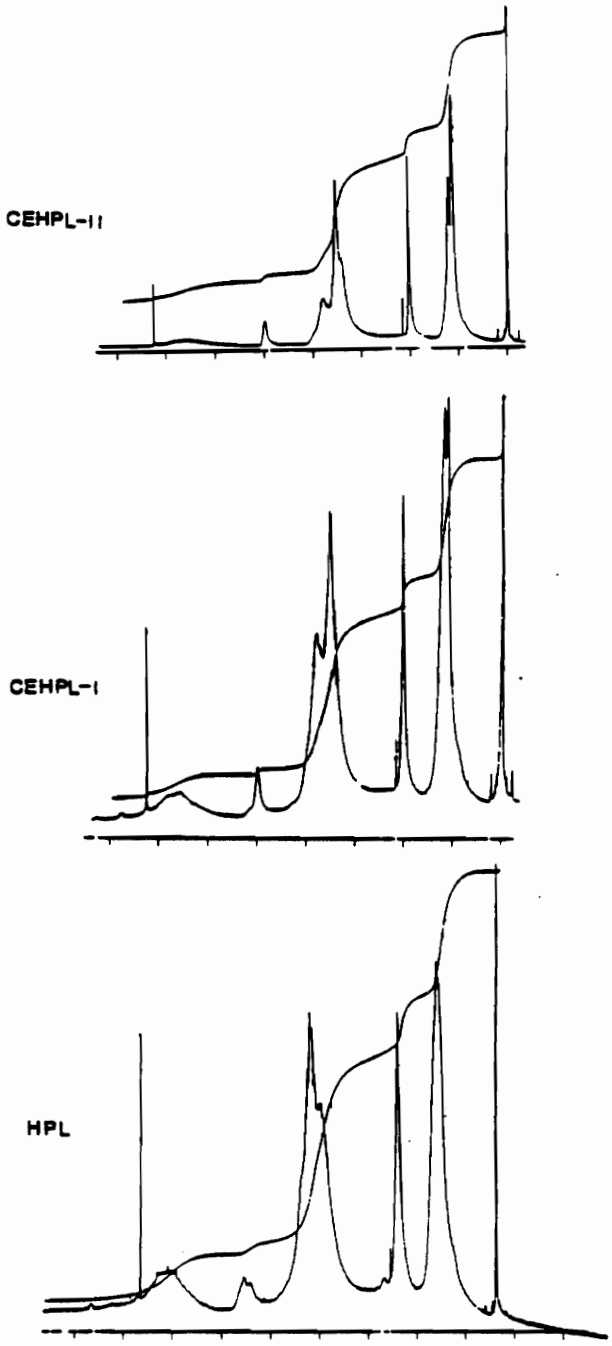

Figure 15. Three typical H-NMR spectra of acetylated HPL and CEHPL at two levels of propoxylation (1.5 and 3.0 gPO/gHPL).

Table 12. Percent Integration in the H-NMR Spectra by Ranges for Acetylated HPL and CEHPL.

Sample	i-Prl/Mel (molar ratio)	Range 2-3 8.0-5.74	Range 4-5 5.79-2.5	Range 6-7 2.5-1.58	Range 8 1.58-09	Range 8'[1*]	Range 8/7	Range 8'/7	PO[2*] units/ arm
0	0.89	19.7	37.6	22.2	20.5	20.5	0.92	0.92	1.0
0-I	2.21	8.2	41.0	16.4	33.6	33.6	2.05	2.05	2.2
0-II	3.43	4.8	35.4	12.2	44.2	44.2	3.62	3.62	3.9
1	0.87	15.8	38.8	21.9	24.0	20.8	1.10	0.95	1.0
1-I	2.14	9.0	41.7	13.9	35.4	32.2	2.55	2.32	2.7
1-II	3.46	9.5	43.8	10.2	34.3	31.1	3.36	3.05	3.6
2	0.83	14.1	42.4	17.7	25.8	20.9	1.46	1.18	1.0
3	0.55	13.8	40.9	17.5	28.3	21.2	1.62	1.21	1.0
3-I	1.66	11.3	44.1	13.0	35.0	27.9	2.69	2.15	2.4
3-II	2.16	9.3	41.2	7.7	35.7	28.6	4.64	3.71	4.2
4	0.76	5.8	29.1	9.7	55.3		5.70		
4-I	1.93	12.0	44.3	11.5	32.8		2.85		
4-II	2.48	7.6	43.9	8.1	38.9		4.80		
5	0.55	12.8	45.6	11.9	29.6	19.6	2.49	1.65	1.0
5-I	1.46	8.7	45.1	9.3	34.6	24.6	3.72	2.65	2.6
5-II	2.21	5.6	44.0	10.1	37.7	27.7	3.73	2.74	2.7
6	0.75	4.7	26.5	9.4	58.8		6.26		
6-I	1.21	7.3	35.2	7.8	43.5		5.58		
6-II	1.25	3.2	37.2	7.0	45.5		6.50		

[1*] Range 8' signals represent range 8 signals minus the proton signals from ethoxyl groups.

[2*] In the calculation of PO units/arm the degree of capping of each HPL was taken in account, as given by the following equation:

$$\#\ \text{PO Units/arm} = \frac{\text{Range 8'/7 of CEHPL}}{\text{Range 8'/ 7 of HPL} * (1\text{-degree of capping})}$$

aromaticity (i.e. signal in range 2) was also observed as a result of chain extension.

The degree of chain extension was determined by taking the ratio between range 8 and range 7 proton signals from the spectrum integration. Since each HPL has an average of 1 propylene oxide unit per arm, which gave a signal ratio of 0.9, the CEHPL value from range 8/ range 7 signal ratio when divided by 0.9 will correspond to the degree of chain extension, or to the number of PO-units linked chain-like to each other in each arm. Thus H-NMR results suggest 2.2 and 4.0 PO-units per arm at the two levels of propoxylation (1.5 and 3.0 g PO/g HPL). These values were in significant agreement with HI/GC results that indicated for the uncapped CEHPL an average of 2.5 and 3.9 PO-units per arm, at each level of propoxylation.

For the capped HPL's and their CEHPL's, the calculation for the degree of chain extension was not straightforward. From the proton signal of range 8, the signal due to methyl protons from the ethoxyl groups must be discounted. The proton signals from range 8 are plotted versus ethoxyl content of the capped HPL in Figure 16. The data indicates a strong linear relationship between proton signal and ethoxyl content ($r = 0.98$). This linearity can be expressed by the equation

$$CH_3 \text{ proton signal} = 20.47 + 1.06 \times \text{ethoxyl content (\%)} \qquad \text{(Eq. 5.2)}$$

This equation produces a factor which discounts the contribution of proton signals due to ethoxyl groups. This factor was determined to be

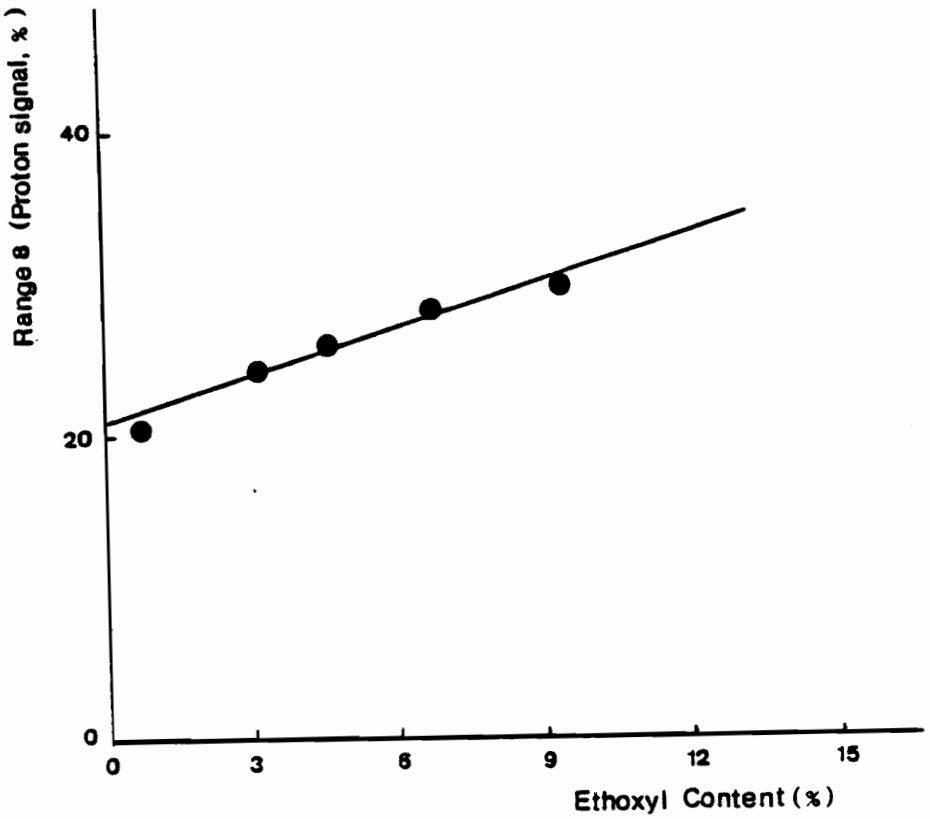

Figure 16. Methyl proton signals from range 8 versus ethoxyl content of capped HPL.

1.06 x ethoxyl content. In other words, for a capped HPL and its respective CEPHL the correction is made by subtracting 1.06 x ethoxyl content of that sample from the percentage of proton signal of range 8. In Table 12 the Range 8' column presents the corrected values after discounting the methyl protons from the ethoxyl groups.

A second factor needs to be considered in the calculation of degree of chain extension. This is related to the degree of capping or the number of arms. For instance, sample #1 (Table 4) has a degree of capping of 11%. This structure, after subtraction of methyl proton signal from ethoxyl groups, gives a range 8'/range 7 signal ratio of 0.95. However, the corresponding CEHPL signal ratio is no more a multiple of this number since the structure is 11% capped. The new value to be considered in the computation is 89% (i.e. 100% - 11%) of 0.95, that is, 0.85. Thus the CEHPL value from range 8'/range 7 signal ratio for sample #1 when divided by 0.85 can be considered as the approximate degree of chain extension, or number of PO units linked chain like to each other in the arm. This approach for the other samples produced almost identical results by H-NMR as by the HI/GC technique. The star-like macromers had accordingly an average of 2.5 and 3.6 PO units/arm at each level of propoxylation.

In this analysis the sample #4 and the 6 were not included. The reason for this is based on the peculiarity of the spectra of these samples (see Figure 17) when compared with the other "normal" capped HPL's. In contrast to the other capped HPL's, both samples presented strong, highly shielded proton signals at low δ -values (ca 0.9 ppm).

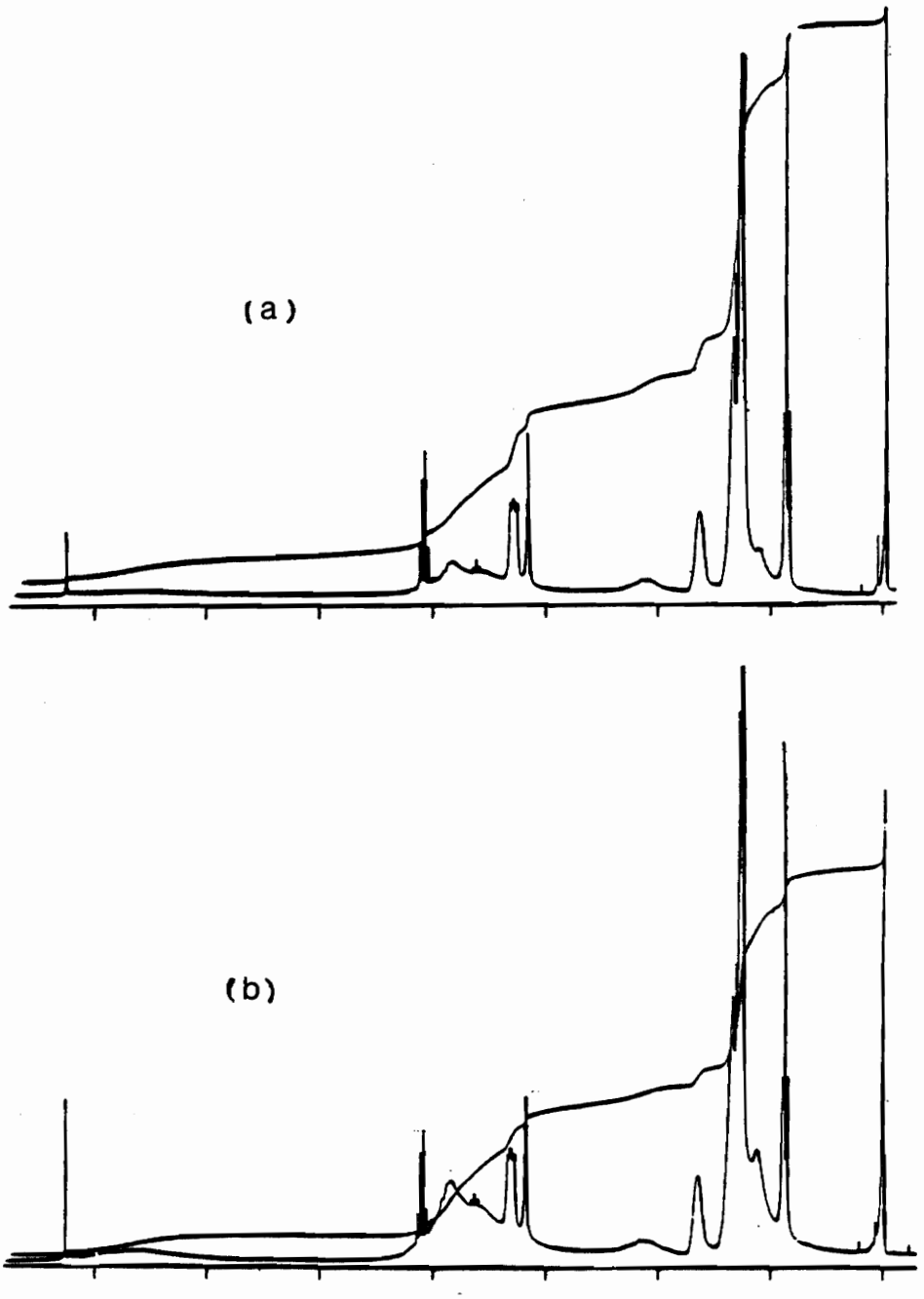

Figure 17. H-NMR spectra of CEHPL #6 (a) and #4 (b).

But the integration of these signals in range 8 gave values (i.e. 55.3 and 58.8%) which were more than double those of the other capped HPL's, (i.e. 20.5 to 29.6%). On the other hand, the aromatic proton signals (i.e. range 2) of these samples are too low (5.8 and 4.7%, respectively) when compared to the "normal" capped HPL's that ranged from 12.0 to 9.7%.

5.4 Thermal Analysis

The results from the determination of glass transition temperatures of HPL, of capped HPL, and of their respective chain extended products are listed in Table 13. The data were obtain from blends with ETPVA, PE or PMMA. The choice of thermoplast was determined by the need of the T_g to be $>20^{o}C$ different from the HPL derivative. Thus, with a highly phase-separated polymer blend it was possible to observe a distinct transition behavior (T_g) of the HPL and its derivatives by using DMTA.

A typical DMTA thermogram of CEHPL blended with 60% ETPVA 18 is shown in Figure 18. The first transition ($T_g = 55^{o}C$) corresponds to CEHPL, and the second ($T_g = -8^{o}C$) to ETPVA 18.

The data reflects a decrease in T_g due to the effect of capping OH groups by ethoxyl groups (see Figure 19). This must probably be attributed to a reduction in hydrogen bonding. As the number of free hydroxyl groups decreases, hydrogen bonding also decreases, thereby lowering the T_g. The low T_g for two of the samples (i.e. #4 and 6) can be explained by the probable presence of solvent since both samples were viscous tars rather than solid powders. The presence of even small

Table 13. Glass Transition Temperature of HPL and CEHPL in 40% Polyblends.

Sample	T_g (°C)
0/ETPVA 18[1*)]	71
0-I/ETPVA 18	35
0-I/PE[2*)]	50
0-II/PMMA[3*)]	23
1/ETPVA 18	37
1-I/ETPVA 18	55
1-I/PE	60
1-II/PE	36
2/ETPVA 18	57
3/ETPVA18	68
3-I/PE	49
3-II/PE	38
4/ETPVA 18	20
4/PE	27
4-I/PE	50
4-II/PE	37
5/ETPVA 18	57
5-I/PE	64
5-II/PE	45
6/ETPVA 18	12
6/PE	32
6-I/PE	42
6-II/PE	42

[1*)] ETPVA 18 indicates 18% vinylacetate commonomer component in ethylene-vinylacetate copolymer

[2*)] Polyethylene

[3*)] Poly (methyl methacrylate)

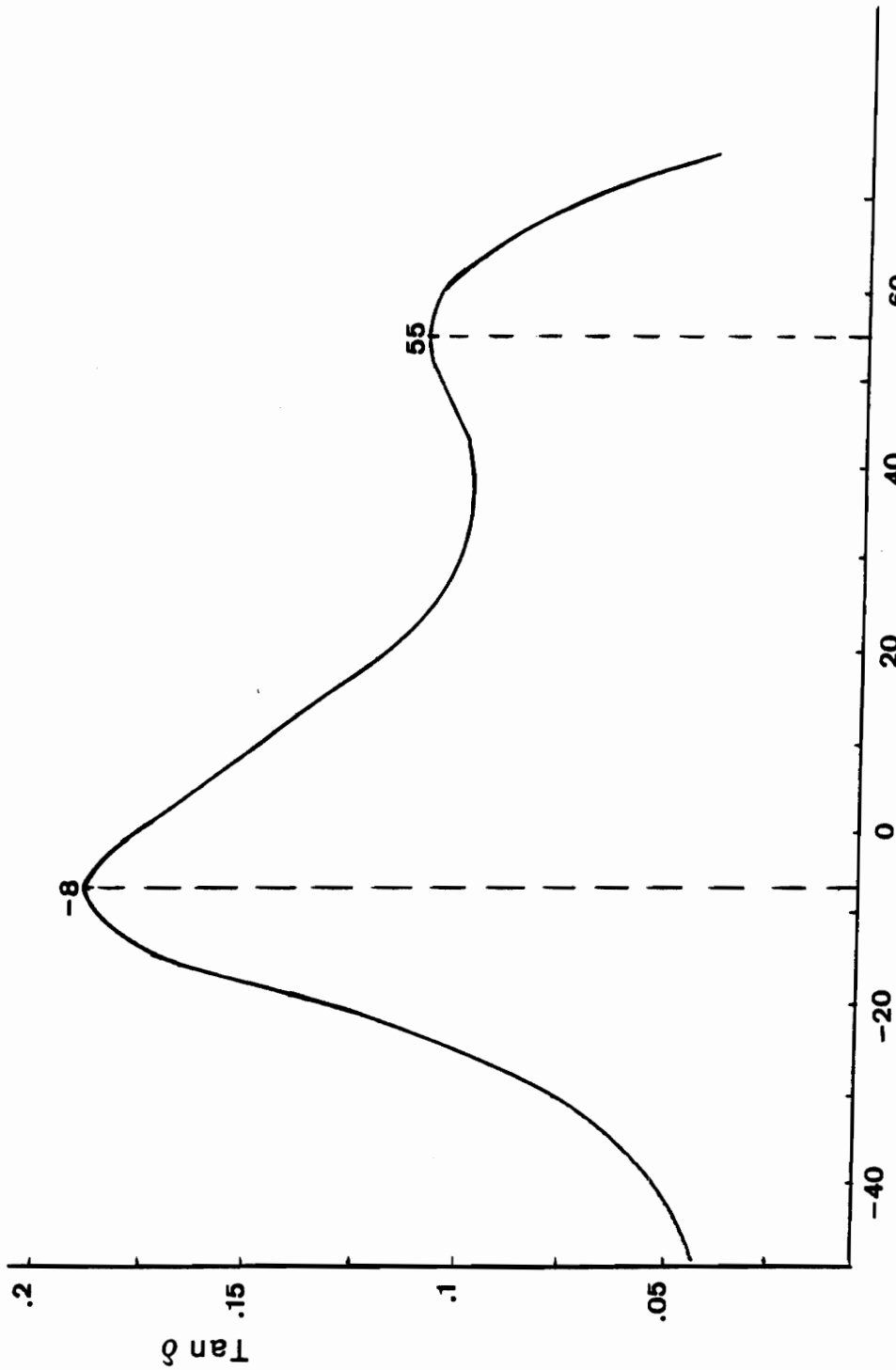

Figure 18. Typical tanδ curve of a blended CEHPL with 60% ETPVA18.

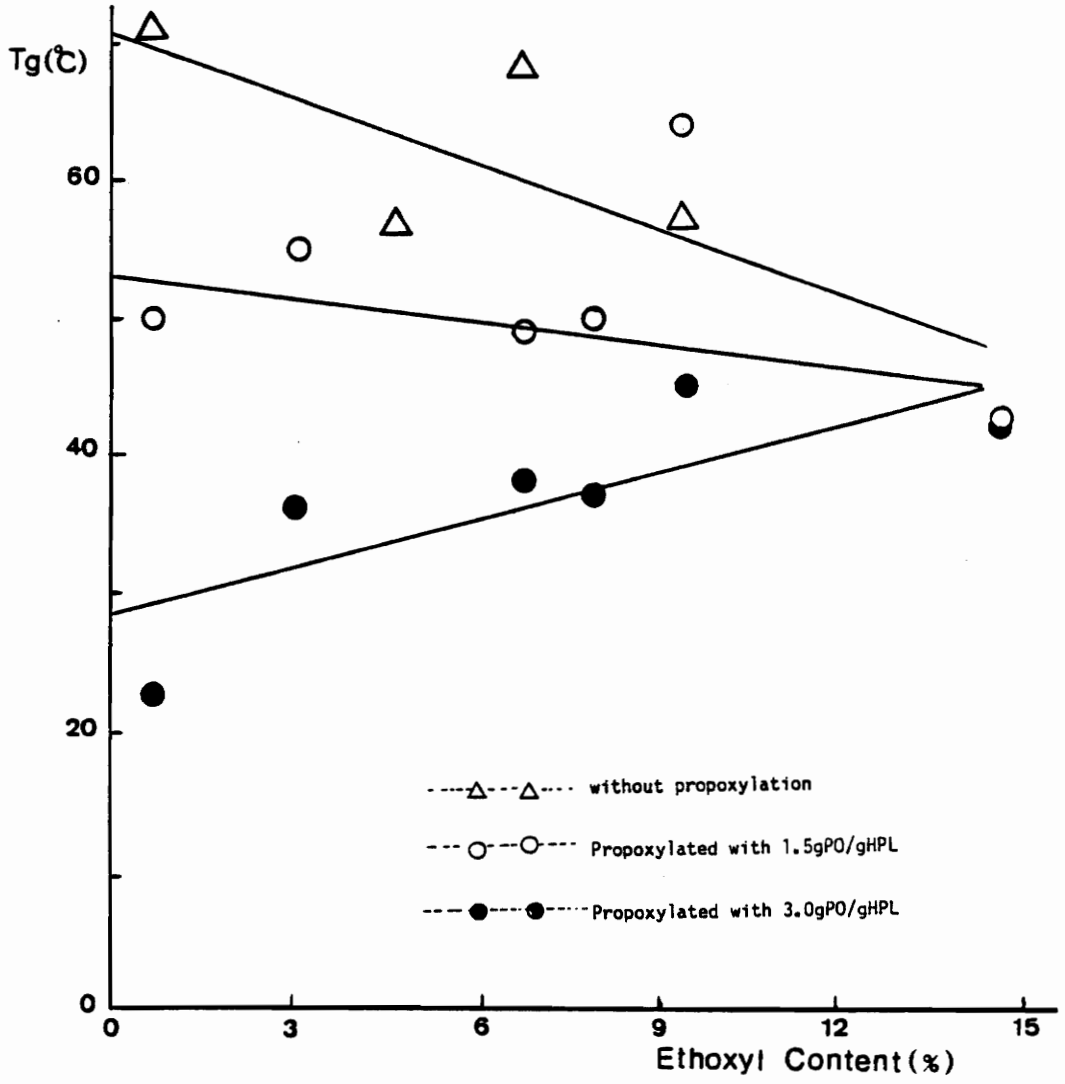

Figure 19. Relationship between T_g and ethoxyl content in CEHPL.

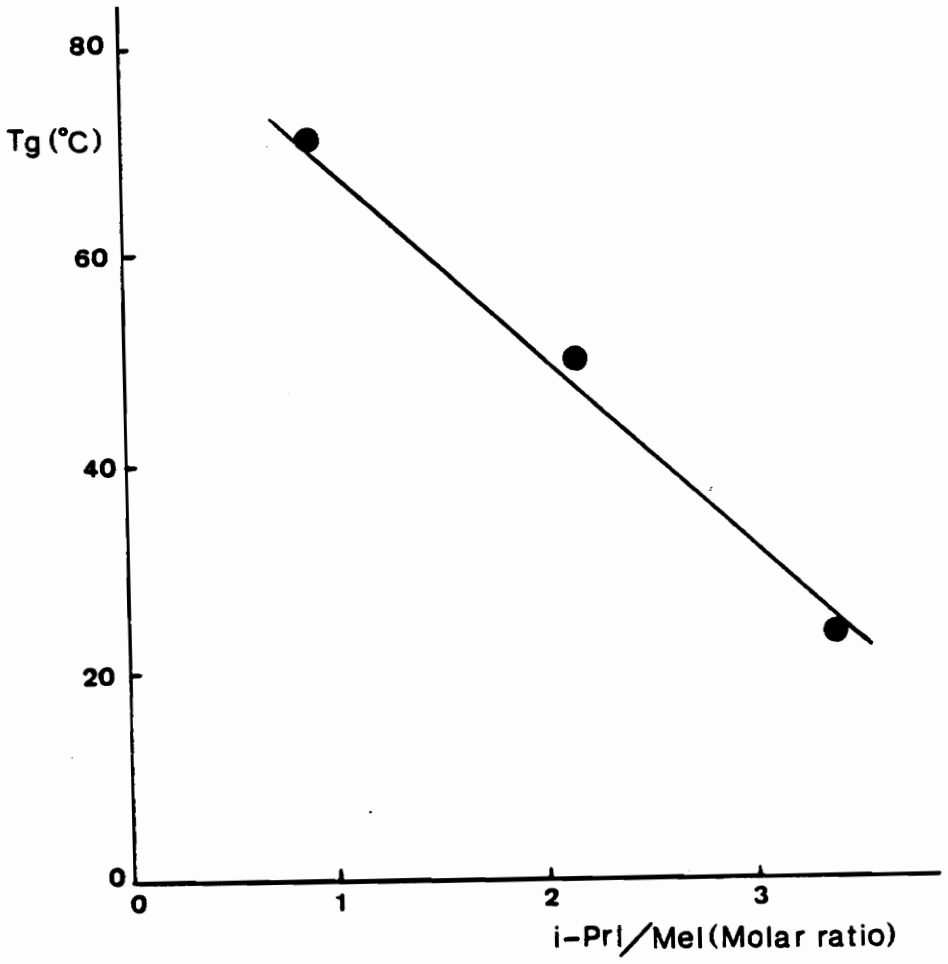

Figure 20. Glass transition temperature versus i-PrI/MeI (molar ratio) for uncapped HPL and chain extended derivatives.

concentrations of diluent (monomer, solvent, H_2O, impurities, etc.) (47) is known to potentially lead to a shift in T_g of over 40°C. Nevertheless, more T_g analysis is required before conclusive reasons for the deviation of the values of 2 samples can be given. The chain extended products, in general, reflected lower T_g-values than their parent uncapped or capped lignin derivatives. Figure 20 presents the relationship between T_g and i-PrI/MeI molar ratio. Although there are only 3 points in the curve, it seems that the higher the degree of propoxylation (higher i-PrI/MeI molar ratio), the lower is the T_g. This agrees with Kelley and other earlier results (25, 45).

5.5 Discussion in Relation to Model Structure

A problem frequently encountered with lignin is related to the complexity of its structure. Lignin is known to be an aromatic, amorphous material, characterized by a considerable content of methoxyl and hydroxyl aliphatic and phenolic groups. Although there are yet many details of lignin structure to be learned, most of its important structural features are probably now known (33).

Various structural models of lignin have been advanced over the years on the basis of in-depth analytical studies (34,35). Figure 21 shows one of the most recent concepts for a softwood lignin structure (35,36). It comprises 94 phenylpropane units, corresponding to a total molecular weight of more than 17,000. The structure is supposed to represent milled wood lignin from loblolly pine (Pinus taeda) and its experimental basis involves elemental analysis, sugar and ash

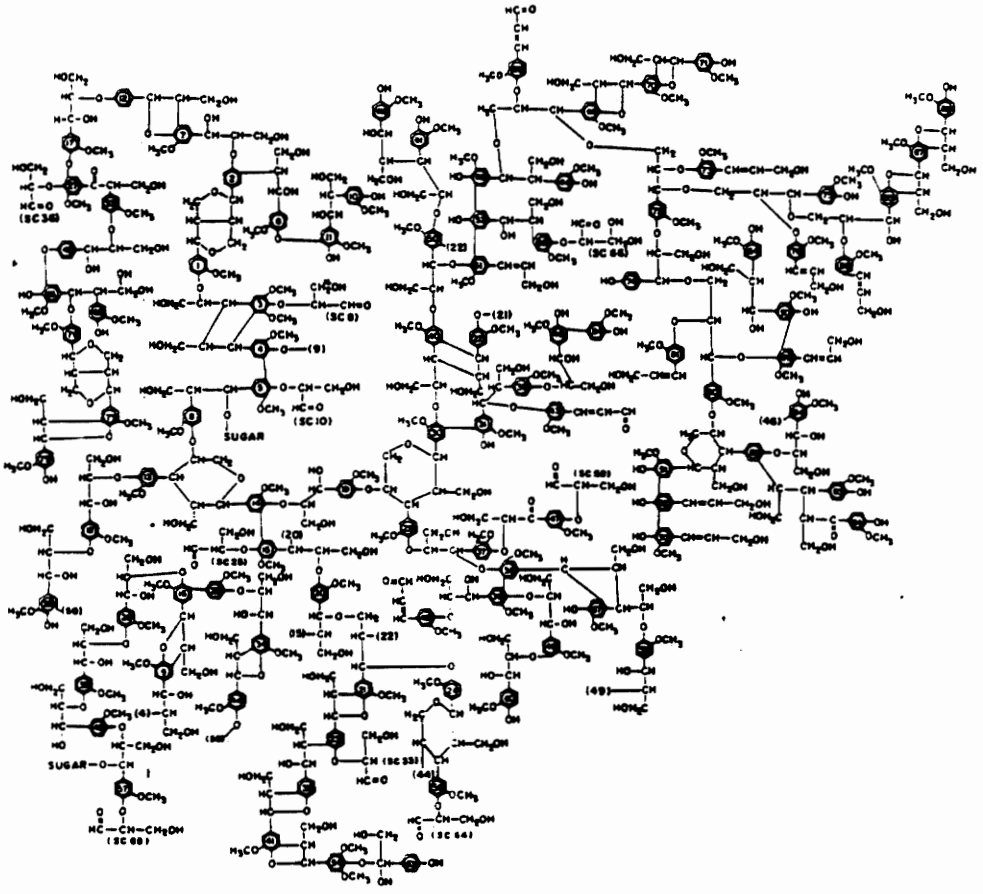

Figure 21. Softwood lignin model designed by computer simulation (35).

determination, H-NMR spectroscopy, permaganate oxidation, and gel permeation chromatography (GPC) (35). This model agrees well with individual analytical procedures and permits the correlation and comparison of structural features with various primary experimental observations (37).

5.5.1 Structural Model for HPL Derivative

Chemical modification of lignin with propylene oxide leads to the formation of hydroxypropyl lignin. Notable properties of these derivatives are their superior solubility in several organic solvents, and their low glass transition temperature when compared to their parent lignin. Based on an evaluation of the synthesis, using model units, and based on a variety of analysis results (8, 9) it is possible to represent experimental findings in a structural model that agrees satisfactorily with primary analytical observations. In order to make some predictions for the kind of results that should be achieved, the HPL structural model shown in Figure 22 was selected. It constitutes the starting point for the theoretical considerations concerned with degrees of capping and chain extension. It permits the prediction of structural characteristics of the star-like macromers in relation to method of treatment.

5.5.2 HI/GC Treatment

Theoretical data with regard to ethoxyl content are shown on Table 14.

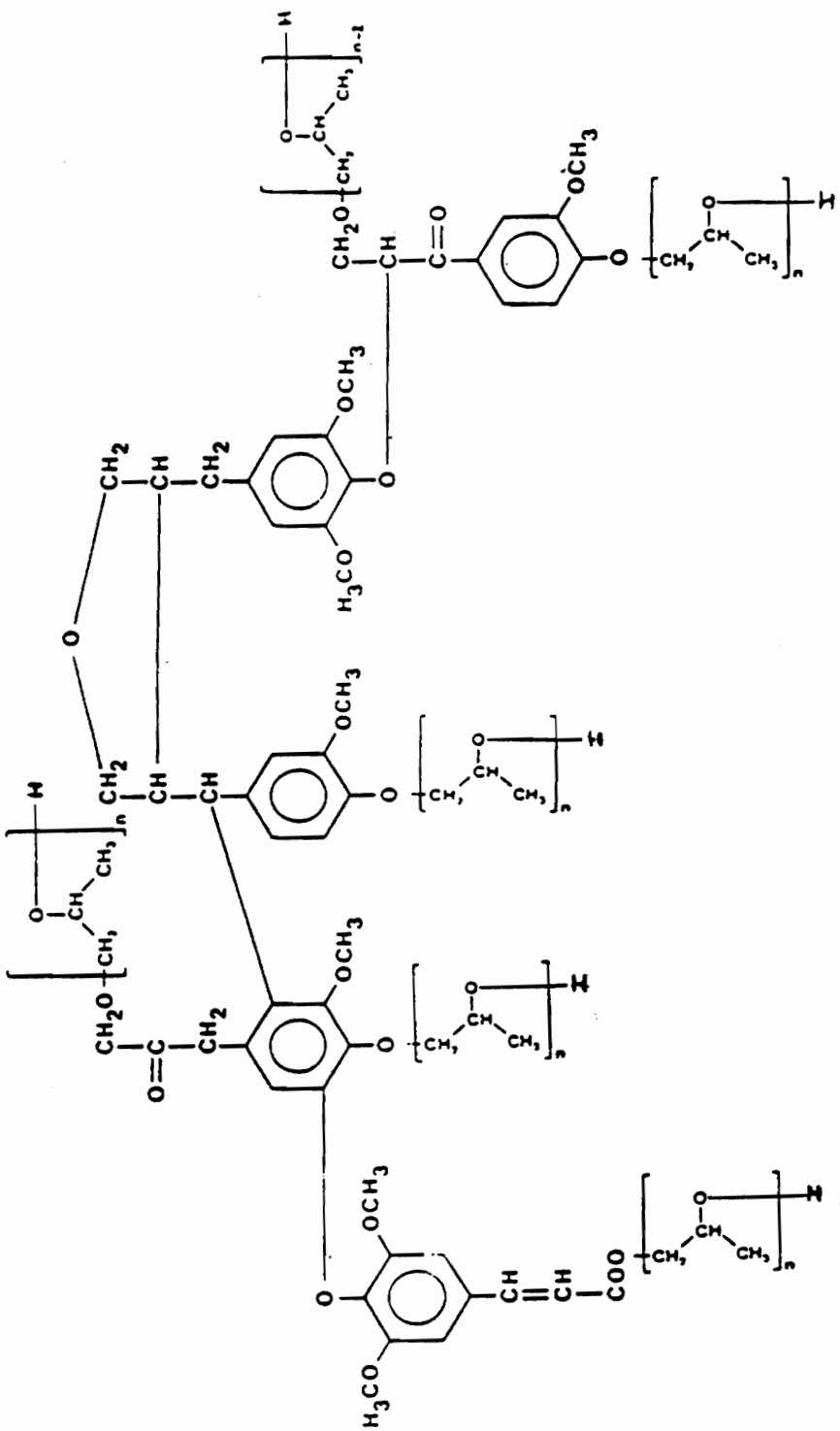

Figure 22. Schematic representation of a hydroxypropyl (organosolv) lignin derivative (n=1).

Table 14. Theoretical Data of Ethoxyl and Hydroxyl Content in a Series of Capped HPL's.

Experiment Number	Number of free OH/$\overline{M}_n$	Number of Ethoxyl Groups	$\overline{M}_n$	Ethoxyl Content(%)	OH Content (%)	OH Content meq/g
1	6	0	1286	0	7.93	4.66
2	5	1	1314	3.42	6.47	3.81
3	4	2	1342	6.71	5.07	2.98
4	3	3	1370	9.85	3.72	2.19
5	2	4	1398	12.88	2.43	1.43
6	1	5	1426	15.78	1.19	0.70
7	0	6	1454	18.57	0	0

The maximum ethoxyl content for this HPL structure was calculated to be 18.57% when all its OH groups were capped. It was assumed in this theoretical consideration that the molar substitution, defined as the number of propylene oxide units linked to another PO unit, would be 5. Thus, considering that the starting HPL or capped HPL has already 1 PO unit (n=1) per arm, the number of PO units resulting from the chain extension reaction will vary from n = 2 to 5.

Table 15 presents theoretical data concerning the average length of arms, number of arms, $\overline{M}_n$ and HI/GC of the star-like macromers. This model is based on several assumptions. The first is that the HPL model has retained one primary hydroxyl group in its structure. This OH site, compared to the secondary OH groups of the propylene oxide in HPL, will generate an arm with one PO unit less than the others, on average. The second is that this same primary OH is the first to be blocked during the capping reaction. Thus, star-like macromers with number of arms lower than 6 will have the same size and length. The third assumption is that the Zeisel-gas chromatography method produces quantitative results on the methoxyl, ethoxyl and isopropoxyl ether contents.

For a better appreciation of the data, a plot of a family of curves relating the i-PrI/MeI molar ratio versus ethoxyl content was drawn (Figure 23). Each line represents a different level of propoxylation expressed as number of PO units per arm or length of arm. In the same graph experimental results were plotted for comparison. It is observed that the ethoxyl content or number of arms of the experimental samples conforms closely with the theoretical data. This indicates that the HPL

Table 15. Theoretical Data Concerning the Average Arm Length, Number of Arms, $\bar{M}_n$ and HI/Gas Chromatogram of HPL and CEHPL.

Samples (ID)	Arm Length (n)	# of arms	$\bar{M}_n$	MeI ($gmol^{-1}$)	i-PrI ($gmol^{-1}$)	i-PrI/MeI (molar ratio)
0-1	1	6	1286	994	850	0.86
0-2	2	6	1634	994	1870	1.88
0-3	3	6	1982	994	2890	2.91
0-4	4	6	2330	994	3910	3.93
0-5	5	6	2678	994	4930	4.96
1-1	1	5	1314	994	850	0.86
1-2	2	5	1604	994	1700	1.71
1-3	3	5	1894	994	2550	2.57
1-4	4	5	2184	994	3400	3.42
1-5	5	5	2474	994	4250	4.28
2-1	1	4	1342	994	850	0.86
2-2	2	4	1579	994	1530	1.54
2-3	3	4	1806	994	2210	2.22
2-4	4	4	2038	994	2890	2.91
2-5	5	4	2270	994	3570	3.59
3-1	1	3	1370	994	850	0.86
3-2	2	3	1544	994	1360	1.37
3-3	3	3	1718	994	1870	1.88
3-4	4	3	1892	994	2380	2.39
3-5	5	3	2066	994	2890	2.91
4-1	1	2	1398	994	850	0.86
4-2	2	2	1514	994	1190	1.20
4-3	3	2	1630	994	1530	1.54
4-4	4	2	1746	994	1870	1.88
4-5	5	2	1862	994	2210	2.22
5-1	1	1	1426	994	850	0.86
5-2	2	1	1484	994	1020	1.03
5-3	3	1	1542	994	1190	1.20
5-4	4	1	1600	994	1360	1.37
5-5	5	1	1658	994	1530	1.54

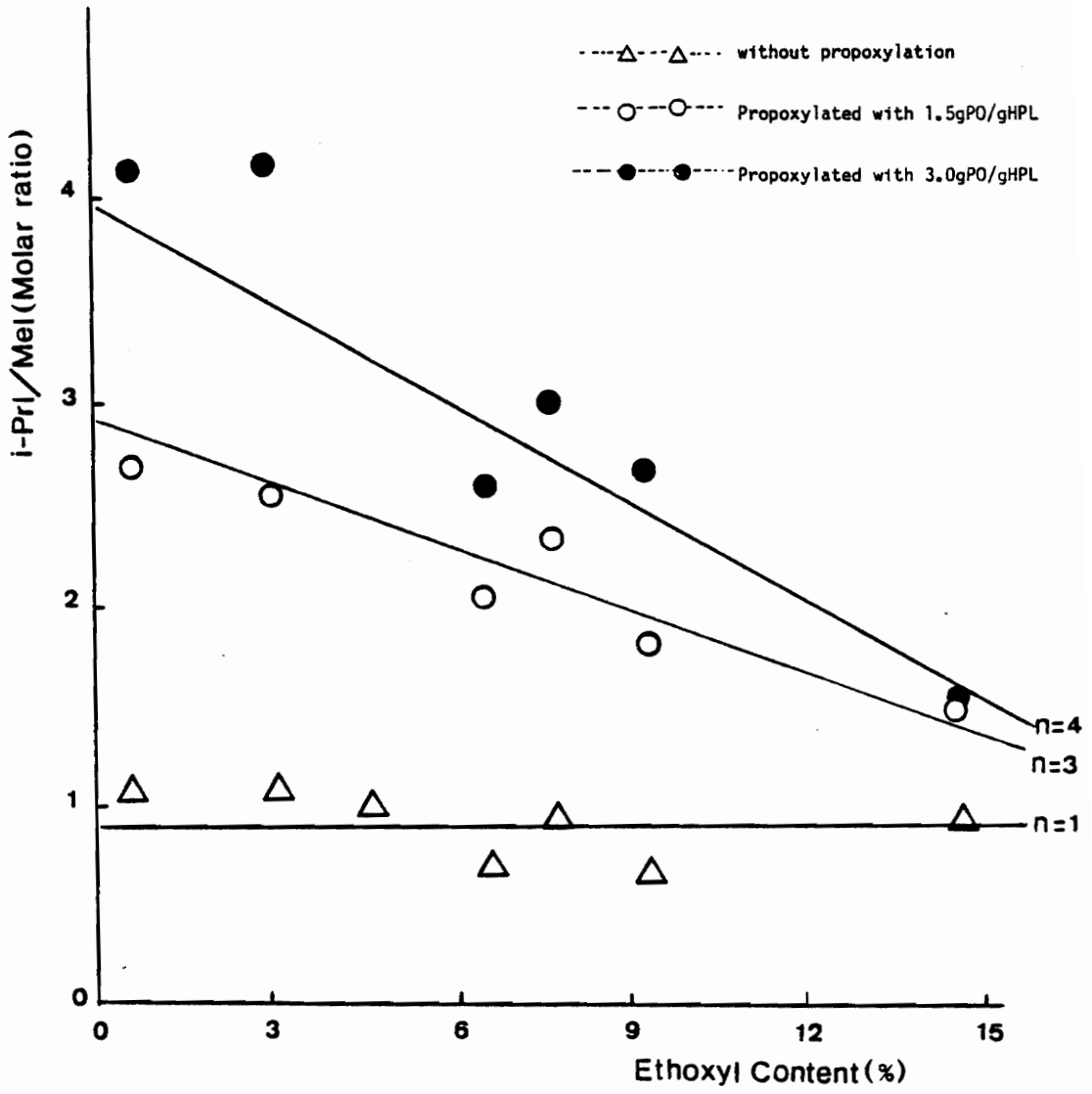

Figure 23. Relationship between i-PrI/MeI (molar ratio) and ethoxyl content in CEHPL with different arm length (n).

has approximately the same number of hydroxyl groups as the structural model. In fact, the OH titration performed on HPL resulted in 8.33% total hydroxyl (see Table 4). This value is very close to the 7.93% suggested by the model of Figure 22. It can also be seen that the experimental results follow the theoretical line. All the data related to HPL and capped HPL without chain extension fit very well on line n=1. The same observation can be made with the respective chain extended samples, but to different degrees. According to the model, those samples extended with 1.5 g PO/g HPL increased the arm length from one to three PO units, while those extended with 3.0 g PO/g HPL presented an average arm length of 4 PO units per arm.

5.5.3 UV Treatment

Based on the assumption that the propylene oxide chains "dilute" the absorbing groups in HPL, it is possible, with the known HPL absorptivity coefficient (i.e., the experimentally determined value of 22.14 L g^{-1} cm^{-1}) and with the HPL structural model, to calculate theoretical absorptivity values for the star-like macromers. This is shown in Table 16. These values are better appreciated when plotted against the ethoxyl content as shown in Figure 24.

Each line corresponds to the number of PO units per arm, or length of arm. The same graph gives the experimental results. A surprisingly good agreement is revealed between the experimental and theoretical data. This means that the HPL model structure can be viewed as a "good (i.e., representative) model" for analytical studies. Although the same

Table 16. Theoretical Absorptivity Coefficients for HPL and CEHPL

Sample (ID)	Arm Length (n)	Number of Arms	$\overline{M}n$	Absorptivity (Lg^{-1} cm^{-1})
0-1	1	6	1286	22.1
0-2	2	6	1634	17.4
0-3	3	6	1982	14.4
0-4	4	6	2330	12.2
0-5	5	6	2678	10.6
1-1	1	5	1314	21.7
1-2	2	5	1604	17.7
1-3	3	5	1894	15.0
1-4	4	5	2184	13.0
1-5	5	5	2474	11.5
2-1	1	4	1342	21.2
2-2	2	4	1574	18.1
2-3	3	4	1806	15.8
2-4	4	4	2038	14.0
2-5	5	4	2270	12.5
3-1	1	3	1370	20.8
3-2	2	3	1544	18.4
3-3	3	3	1718	16.6
3-4	4	3	1892	15.0
3-5	5	3	1066	13.9
4-1	1	2	1398	10.4
4-2	2	2	1514	18.8
4-3	3	2	1630	17.5
4-4	4	2	1746	16.3
4-5	5	2	1862	15.3
5-1	1	1	1426	20.0
5-2	2	1	1484	19.2
5-3	3	1	1542	18.5
5-4	4	1	1600	17.8
5-5	5	1	1658	17.2

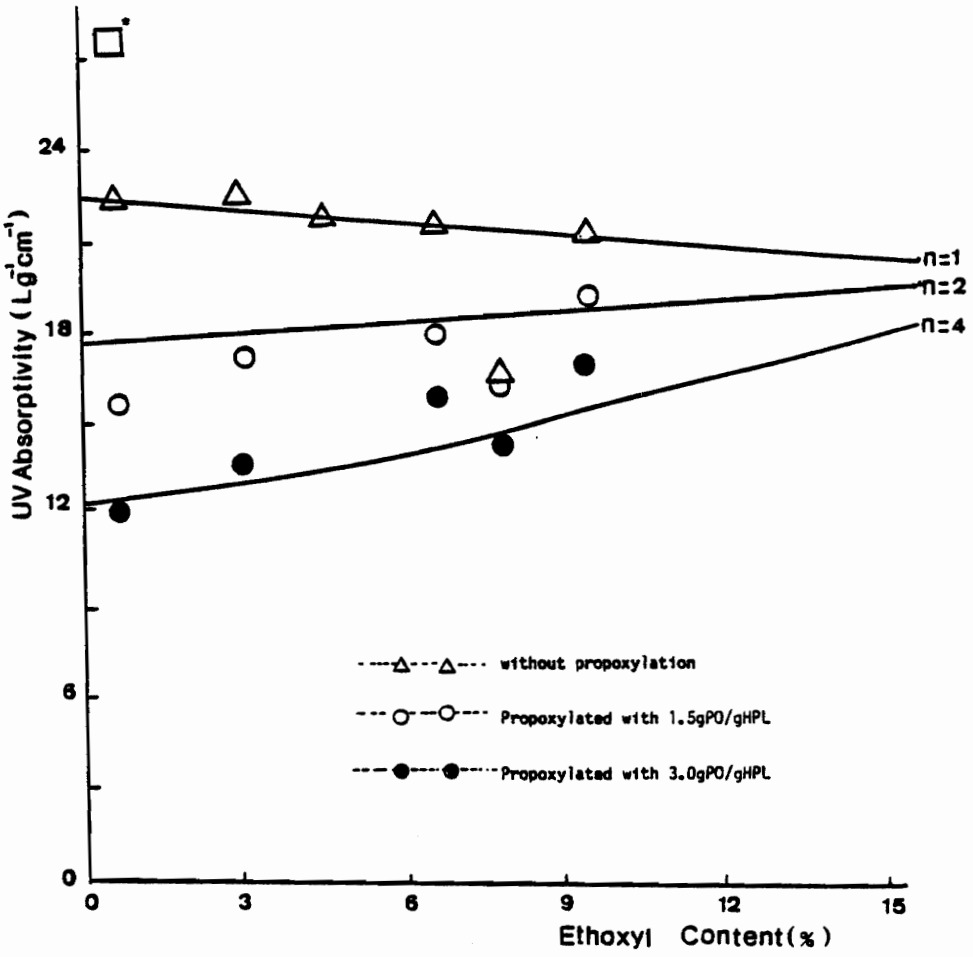

Figure 24. Relationship between absorptivity coefficient and ethoxyl content in CEHPL with different arm length (n).

* organosolv lignin

absorptivity coefficient has arbitrarily been established for the model, the other points in the curve, on the other hand, agree very well with the predicted data for n=1 for HPL and for capped HPL without chain extension.

Another important observation concerns the chain extended samples. Two levels of propoxylation can clearly be seen. On the first level are those samples that were obtained from the reaction using 1.5 g PO/capped HPL. All the experimental points stayed between lines 2 and 3, and this indicates that an average degree of chain extension of between 2 and 3 PO units per arm was achieved. On the second level of propoxylation, when the amount of PO doubled, the data show an increase in arm length of the same proportion, that is, an average of between 4 and 5 PO units per arm. A curious observation is that the number of arms has apparently no influence on the length of arms. All star-like macromers, produced under identical reaction conditions, produced the same length of arms, irrespective of the number of arms.

5.5.4 H-NMR Treatment

Table 17 presents the hypothetical distribution of protons in ranges 7 and 8 for acetylated HPL, for capped HPL, and for their respective CEHPL derivatives based on the HPL structure model. The ratio between ranges 8 and 7 versus ethoxyl content was plotted in Figure 25. Each curve on the graph corresponds to a different arm length (n) of the star-like macromer. The experimental results were plotted on the same graph. A good agreement is revealed between

Table 17. Hypothetical H-Distribution in Ranges 7 & 8 for Acetylated HPL and CEHPL.

Sample (ID)	Arm length (n)	Number of arms	Range 7 Number of H from O-Acetyl	Range 8 Number of H from $PO(CH_3)$ and $Et(CH_3)$		Range 8 / Range 7
0-1	1	6	18	15	0	0.8
0-2	2	6	18	33	0	1.8
0-3	3	6	18	51	0	2.8
0-4	4	6	18	69	0	3.8
0-5	5	6	18	87	0	4.8
1-1	1	5	15	15	3	1.2
1-2	2	5	15	30	3	2.2
1-3	3	5	15	45	3	3.2
1-4	4	5	15	60	3	4.2
1-5	5	5	15	75	3	5.2
2-1	1	4	12	15	6	1.7
2-2	2	4	12	27	6	2.7
2-3	3	4	12	39	6	3.7
2-4	4	4	12	51	6	4.7
2-5	5	4	12	63	6	5.7
3-1	1	3	9	15	9	2.7
3-2	2	3	9	29	9	3.7
3-3	3	3	9	33	9	4.7
3-4	4	3	9	42	9	5.7
3-5	5	3	9	51	9	6.7
4-1	1	2	6	15	12	4.5
4-2	2	2	6	21	12	5.5
4-3	3	2	6	27	12	6.5
4-4	4	2	6	33	12	7.5
4-5	5	2	6	39	12	8.5
5-1	1	1	3	15	15	10.0
5-2	2	1	3	18	15	11.0
5-3	3	1	3	21	15	12.0
5-4	4	1	3	24	15	13.0
5-5	5	1	3	27	15	14.0

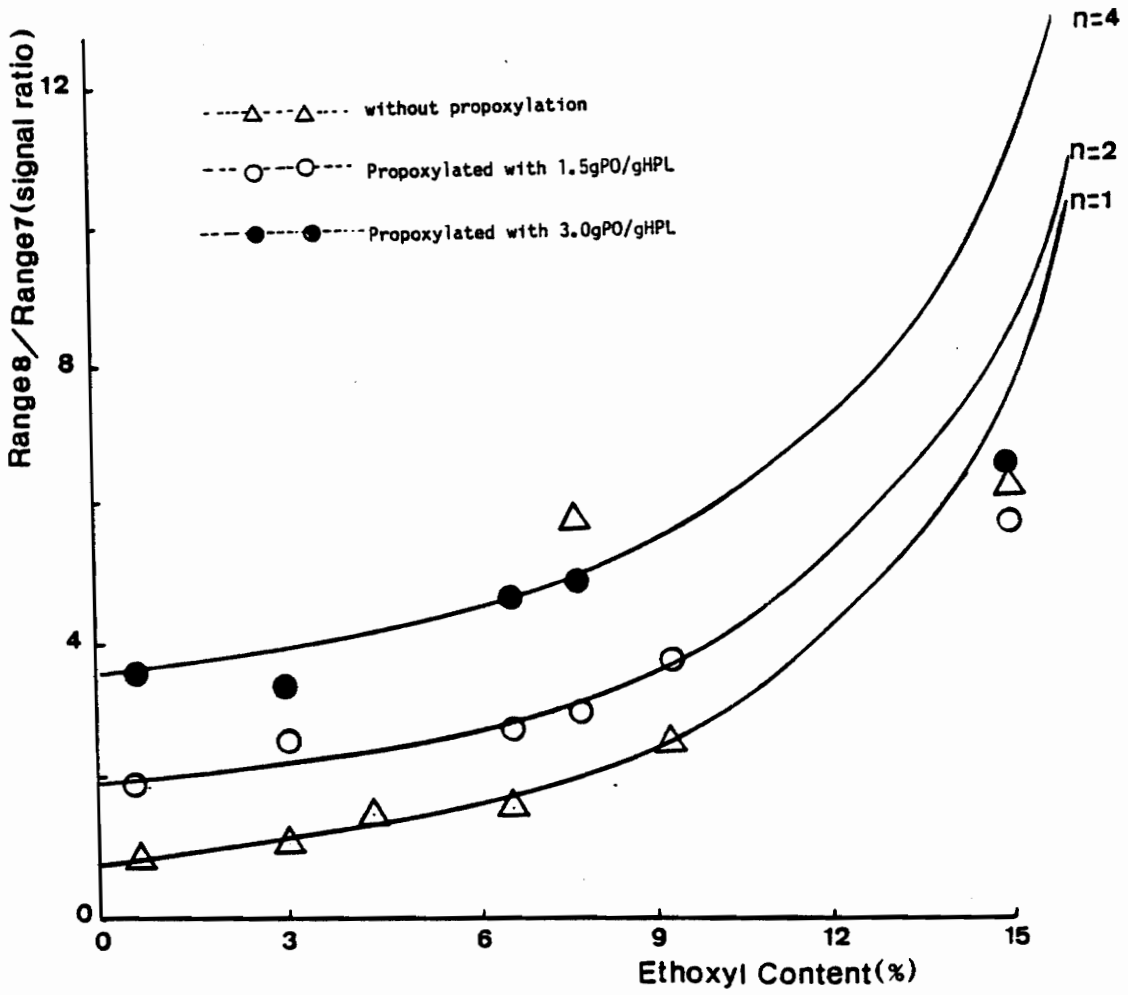

Figure 25. Relationship between methyl proton signal ratio (ranges 8 & 7) versus ethoxyl content in CEHPL with different arm length (n).

theoretical and experimental results. This agreement is more pronounced for the HPL and capped HPL without chain extension. Almost all results fit on the predicted line n=1 for these unextended products. The only exception is the HPL with 7.6% of ethoxyl content (sample #4) which consistently has presented different values than expected in other analysis methods. Again, it is possible to see two distinct levels of chain extension. On the first level an average of between 2 and 3 PO units per arm was achieved while on the second approximately 4 PO units per arm were reached. It can also be said that the experimental values agree with the theoretical up to a degree of capping of around 9% of ethoxyl content. The chain extended samples from the capped HPL with 15% of ethoxy content present lower than predicted results. The reason is probably a consequence of the difficulty that arises from the peak integration when the OH content in the sample is low. Since the OH percentage decreases, the O-acetyl proton signals become less intense, and this makes the integration difficult. Thus, below 9% ethoxyl content, for each level of propoxylation, the star-like macromers with 6, 5 and 4 arms have identical arm lengths.

5.5.5 Thermal Analysis Treatment

In analogy to the approach of the previous sections, theoretical T_g data were calculated according to the Gordon-Taylor equation. The Tg assumed for the HPL model was the same that was determined experimentally. For the capped HPL, the T_g values were also arbitrarily taken from the experimental results based on observed decrease in T_g as

a result of an increase in the degree of capping. The adjustable constant (K) of the Gordon-Taylor equation was taken from a procedure described elsewhere (26).

Table 18 presents the calculated T_g values for HPL, capped HPL and CEHPL based on the Gordon-Taylor equation. T_{g1} and w_1 refer to polypropylene oxide transition temperature and weight fraction monomer, while T_{g2} and w_2 refer to HPL or capped HPL glass transition temperature and weight fraction of HPL.

The calculated T_g's are plotted versus ethoxyl content in Figure 26. Each line on the graph represents the number of PO units linked to each other, or the arm length. Experimental results are plotted in the same graph for comparison. Despite the need for a variety of assumptions a reasonably good fit to the Gordon-Taylor equation for the chain extended samples was achieved. The experimental results follow roughly the theoretical lines. Again, the results show two distinct levels of propoxylation: one at n=2 and the other at n=4.

Table 18. Predicted T_g for HPL and CEHPL. (According to Equation 2.5[1*])

Sample (ID)	Arm length (n)	Number of arms	w_1	T_{g1} (°C)	w_2	T_{g2} (°C)	T_g (°C)
0-1	1	6	-	-75	1	71	-
0-2	2	6	0.2130	-75	0.7870	71	55.1
0-3	3	6	0.3512	-75	0.6488	71	42.4
0-4	4	6	0.4481	-75	0.5519	71	31.9
0-5	5	6	0.5198	-75	0.4802	71	23.2
1-1	1	5	-	-75	1	65.5	-
1-2	2	5	0.1808	-75	0.8192	65.5	52.8
1-3	3	5	0.3062	-75	0.6938	65.5	42.2
1-4	4	5	0.3984	-75	0.6016	65.5	33.2
1-5	5	5	0.4689	-75	0.5311	65.5	25.6
2-1	1	4	-	-75	1	61.0	-
2-2	2	4	0.1474	-75	0.8526	61.0	51.2
2-3	3	4	0.2569	-75	0.7431	61.0	42.7
2-4	4	4	0.3415	-75	0.6585	61.0	35.3
2-5	5	4	0.4088	-75	0.5912	61.0	28.7
3-1	1	3	-	-75	1	57	-
3-2	2	3	0.1127	-75	0.8873	57	49.9
3-3	3	3	0.2026	-75	0.7974	57	43.4
3-4	4	3	0.2759	-75	0.7241	57	37.7
3-5	5	3	0.3369	-75	0.6631	57	32.4
4-1	1	2	-		1	52.8	-
4-2	2	2	0.0766	-75	0.9234	52.8	48.2
4-3	3	2	0.1423	-75	0.8577	52.8	43.9
4-4	4	2	0.1993	-75	0.8007	52.8	39.9
4-5	5	2	0.2452	-75	0.7548	52.8	36.5
5-1	1	1	-		1	49	-
5-2	2	1	0.0391	-75	0.9609	49	46.8
5-3	3	1	0.0752	-75	0.9248	49	44.0
5-4	4	1	0.1088	-75	0.8913	49	42.5
5-5	5	1	0.1399	-75	0.8601	49	40.5

[1*]The K-factor was 0.45.

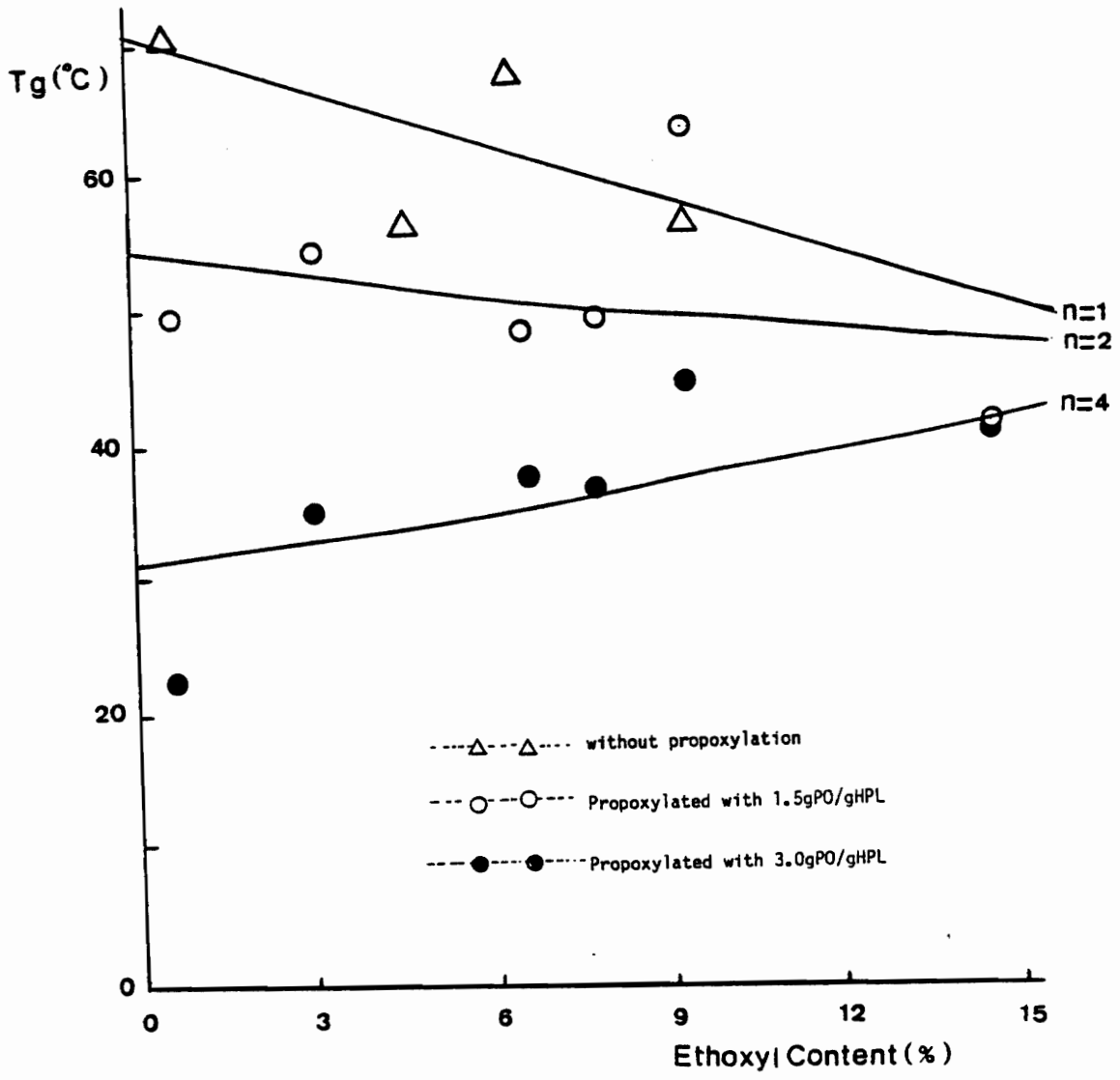

Figure 26. Relationship between T_g and ethoxyl content in CEHPL with different arm length (n).

VI. CONCLUSIONS

Star-like macromers from hydroxypropyl lignin, synthesized by a sequence of capping and chain extension reactions can be analyzed regarding number and length of arms radiating from each monomer.

Six methods of analysis were applied for a quantitative characterization of the star-like macromer.

Hydriodic acid/gas chromatography proved to be the most appropriate for quantitative information about the degree of capping, since it was the only method, among those investigated, that permitted the characterization of HPL derivatives according to their respective alkoxyl groups. Thus, the degree of capping (related to ethoxyl content) of the star-like macromer could only be analyzed by HI/GC. Based on this method it was possible to distinguish and classify star-like macromers with an average of 6, 5, 4 and 2 radiating arms per average macromer. This technique could also determine the macromer arm length. Star-like macromers with an average of 2.5 and 3.5 PO-units per arm were obtained.

Ultraviolet spectroscopy was the simplest and the most rapid method of analysis investigated. The decrease in CEHPL absorptivity coefficient can be attributed to the increase of non-UV absorbing mass after capping and/or chain extension. However, due to the lack of a quantitative relationship between absorptivity coefficient and CEHPL composition (in terms of moles of propylene oxide chain), the results could not be used for the determination of the degree of chain extension.

H-NMR spectroscopy can be a useful method of analysis for the determination of the arm length in star-like macromers. The number of PO-units linked to each other can be calculated from the proton signal ratio between range 8 and range 7. The experimental results demonstrate star-like macromers with 2.2-2.7 and 2.7-4.2 PO-units per arm were obtained, at two levels of propoxylation.

DMTA revealed a decrease in T_g as a consequence of an increase in chain length; however, experimental values were extremely variable.

The HPL structural model used for theoretical calculation once more produced satisfactory agreement with the analytical observations resulting from the methods applied, and thus can be considered an appropriate model for organosolv HPL.

REFERENCES

(1) D.W. Goheen and C.H. Hoyt, Encyclopedia of Chemical Technology, 14, 294 (1981).

(2) S.I. Falkehag, Appl. Polym. Symp., 28, 247-257 (1975).

(3) K. Kringstad, in: Future Sources of Organic Raw Materials-CHEMRAWN I, L.E. St. Pierre and G.R. Brown, eds., p. 627, 1980, Pergamon Press, New York.

(4) V.P. Saraf and W.G. Glasser, J. Appl. Polym. Sci., 29, 1831 (1984).

(5) P.C. Muller and W.G. Glasser, Biotechnology and Bioengineering Symp.., No. 13, 481 (1983).

(6) W.G. Glasser, L. C. -F. Wu, and J. F. Selin, in: Wood and Agricultural Residues - Research on Use for Feed, Fuels and Chemicals, E. J. Soltes, Ed., Academic, New York, 1983, pp. 149-166.

(7) Technology, September 24, 1984 C&N, pp. 19-20.

(8) W.G. Glasser and L.C.F. Wu, J. Appl. Polym. Sci, 29, 1111 (1984).

(9) W.G. Glasser, C. A. Barnett, T. G. Rials, and V. P. Saraf, J. Appl. Polym. Sci., 29, 1815 (1986).

(10) T.G. Rials and W. G. Glasser, Holzforschung 38(4):191-199.

(11) T.G. Rials and W. G. Glasser, Holzforschung 38(5):263-269 (1984).

(12) V.P. Saraf, W. G. Glasser, G. L. Wilkes, and J. E. McGrath, J. Appl. Polym. Sci., 30, 2207 (1985).

(13) D.N. Schultz and D.P. Tate, Encyclopedia of Chemical Technology, 6, 798 (1979).

(14) J.E. McGrath in Block Copolymers Science and Technology, MMI Press Symp. Se. Vol 3., edited by D.J. Meir, Michigan Molecular Inst., p. 1-16 (1979).

(15) L.H. Perling, Recent Advances in Polymer Blends, Grafts, and Blocks, Plenum Press, N.Y. and London, 1979.

(16) B.R.M. Gallot, Adv. Polym. Sci., 19, 85 (1978).

(17) L.K. Bi and L. J. Fetters, Macromolecules, 9, 732 (1976).

(18) R.N. Young and L.J. Fetters, Macromolecules, 11, 899 (1978).

(19) M. Daoud and J.P. Cotton, J. Physique, 43, 531 (1982).

(20) P.A. Small, Adv. Polym. Sci., 18, 1 (1975).

(21) G. Riess, G. Hurtrez and P. Bahadur, Encyclopedia of Polymer Science and Engineering, 2, 324 (1985).

(22) O.H.-H. Hsu and W. G. Glasser, Appl. Polym. Symp., No. 28, 297 (1975).

(23) W. G. Glasser, J. -F. Selin, P. L. Hall, and S. W. Drew, in: Proceedings of the International Symposium on Wood and Pulping Chemistry (Ekman Days), Stockholm, Sweden, 1981, Vol. 4, p. 39.

(24) W. G. Glasser, O. H. -H, Hsu, D. L. Reed, R. C. Forte, and L. C. -F Wu, in: Urethane Chemistry and Applications, K. Edwards, Ed., ACS Symposium Series No. 172, American Chemical Society, Washington, D.C., 1981, p. 311.

(25) S. Kelley, Ph.D. Dissertation, Virginia Tech, 1986.

(26) P.V. Saraf, W.G. Glasser, G.L. Wilkes and J.E. McGrath, J. Appl. Polym. Sci., 30, 2207 (1985).

(27) P.V. Saraf, W.G. Glasser and G.L. Wilkes, J. Appl. Polym. Sci., 30, 2809 (1985).

(28) N. Morohoshi, Bulletin of the Experiment Forest, Tokyo University of Agriculture and Technology, No. 10, p. 183-194.

(29) K.L. Hodges, W. E. Kester, D. L. Wiederrich, and J. A. Grover, Anal. Chem., 51 (13), 2172 (1979).

(30) J.C. Bowman and G.T. Battaglini, Research & Development, Sept. 1985, p. 104-106.

(31) K.V. Sarkanen and C.H. Ludwig, Lignin, Wiley-Int., New York, 1971.

(32) H.H. Jaffee and M. Orchin, Theory and Applications of Ultraviolet Spectroscopy, Wiley, New York, 1962.

(33) R.L. Crawford, Lignin Biodegradation and Transformation, John Wiley and Sons, USA, 1981.

(34) F.E. Brauns and D.A. Brauns, The Chemistry of Lignin: Supplement Volume, Academic Press, London, 1960.

(35) D.F. Fengel and G. Wegner, Wood: Chemistry, Ultrastructure, Reactions, Walter de Gruyter, Berlin, 1984.

(36) W.G. Glasser and H.R. Glasser, Paperi ja Puu, 63(2),71 (1981).

(37) W.G. Glasser, H. R. Glasser, and N. Morohoshi, Macromolecules, 14, 253 (1981).

(38) B.L. Browning, Methods of Wood Chemistry, Interscience Publishers, Vol. II, 1967.

(39) D.N.S. Hon and W.G. Glasser, Polym. Plast. Technol. Eng., 12, 159 (1979).

(40) C.H. Ludwig, B. J. Nist, and J. L. McCarthy, J. Am. Chem. Soc., 86, 1196 (1964).

(41) T. Murayama, "Dynamic Mechanical Properties" in Encyclopedia of Polymer Science and Engineering, Vol. 5, 299 (1986).

(42) M. Gordon and J.S. Taylor, J. Appl. Chem., 2, 493 (1952).

(43) F.W. Billmeyer, Textbook of Polymer Science, John Wiley & Sons, 3rd. edition, 1984.

(44) Nieh W., M.S. Thesis, Virginia Tech, 1986.

(45) P. L. Hall, W. G. Glasser and S. W. Drew, Lignin Biodegradation-Microbiology, Chemistry, and Potential Applications, Vol. II, T. K. Kirk, T. Higuchi, and H. -M. Chang, eds., CRC Press, Inc., pp. 33-49 (1980).

(46) Personal communication C.A. Barnett, Virginia Tech, 1986.

(47) W. A. Lee and R. A. Rutherford. The Glass Transition Temperatures of Polymer, in: Polymer Handbook, J. Brandrup, E. H. Immergut, and W. McDonald, eds., John Wiley & Sons, Inc., 2nd edition, 1975, p. III-139. 1975.

VITA

Willer de Oliveira was born as first son to Mr. and Mrs. Joao Durval de Oliveira on March 9, 1954, in Rio de Janeiro, Brazil. In December 1976, he completed his Bachelor of Science degree in Chemistry at Rio de Janeiro Federal University. While working as a Research Chemist at the Foundation for Industrial Technology he completed a B.S. degree in Chemical Engineering at Rio de Janeiro State University in December, 1980.

His work experience includes 8 years as a Research chemist at the Foundation for Industrial Technology. In this institution he has been conducting research on lignin utilization, sugar cane bagasse and biomass residues.

In September 1985 he received a scholarship for graduate studies in Forest Products at Virginia Polytechnic Institute and State University (VPI&SU) from the Brazilian Government (CNPq).

He married Marilia F.T. Oliveira in May 1982 and had two children, Guilherme and Fernanda.

W. Willer de Oliveira